Electronic Supplementary Material (ESI) for Dalton Transactions.
This journal is © The Royal Society of Chemistry 2021

Impact of the Ferrocenyl Group on Cytotoxicity and KSP Inhibitory Activity of Ferrocenyl Monastrol Conjugates

Anna Wieczorek-Błauż,[a] Karolina Kowalczyk,[a] Andrzej Błauż,[b] Anna Makal,[c] Sylwia Pawlędzio,[c] Chatchakorn Eurtivong,[d,e] Homayon J. Arabshahi,[f] Jóhannes Reynisson,[f,g] Christian G. Hartinger,[f] Błażej Rychlik,[b] Damian Plażuk[a]*

[a] Department of Organic Chemistry, Faculty of Chemistry, University of Łódź, Tamka 12, 91-403 Łódź, Poland

[b] Cytometry Lab, Department of Molecular Biophysics, Faculty of Biology and Environmental Protection University of Łódź, Pomorska 141/143, 90-236 Łódź, Poland

[c] Laboratory for Structural and Biochemical Research, Biological and Chemical Research Centre, Department of Chemistry, University of Warsaw, ul. Żwirki i Wigury 101, 02-089 Warszawa, Poland

[d] Program in Chemical Science, Chulabhorn Graduate Institute, Chulabhorn Royal Academy, Bangkok 10210, Thailand

[e] Center of Excellence on Environmental Health and Toxicology (EHT), Commission on Higher Education (CHE), Ministry of Education, Bangkok 10400, Thailand

[f] School of Chemical Sciences, University of Auckland, Auckland 1142, New Zealand

[g] School of Pharmacy and Bioengineering, Keele University, Staffordshire ST5 5BG, United Kingdom

Table of Contents

[100]

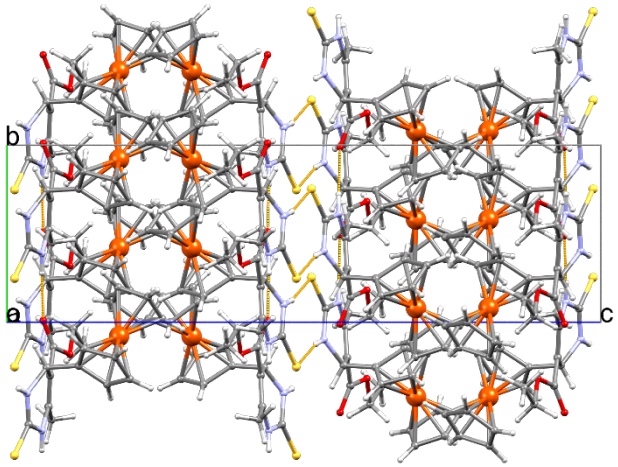

[010]

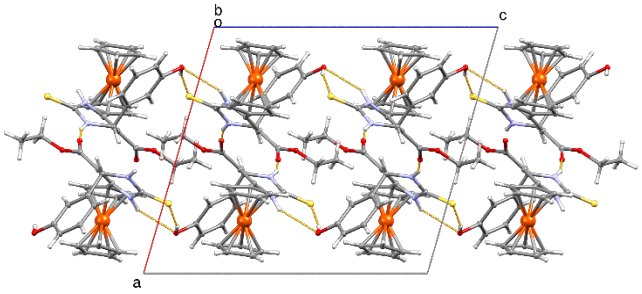

[010]

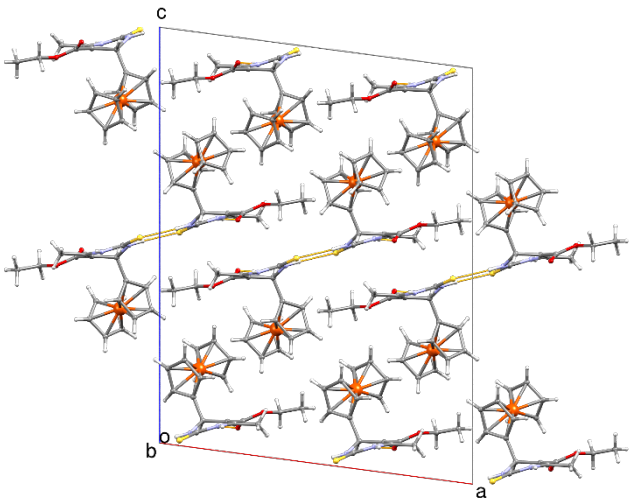

[001]

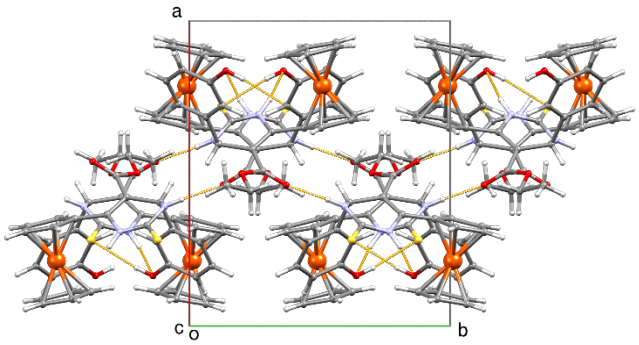

Supporting Figure S1. Selected views of the crystal packing of **4a** (left) and **6a** (right).

Docking studies

The KSP crystal structure derived from Homo sapiens was obtained from the Protein Data Bank (PDB ID: 1Q0B).[1] The co-crystallized ligand (*S*)-**1** was removed and re-docked to the allosteric site with excellent docking overlay (RMSD = 0.532 Å). The co-crystallized ligand, and its re-docked configuration, showed the phenol group deeply buried in the hydrophobic cavity (Supporting Figure S2). The cavity is populated with hydrophobic amino acids Trp127, Ala133, Ile136, Pro137, Tyr211 and Leu214, which form favorable hydrophobic contacts with aromatic phenol and the tetrahydropyrimidine core. Hydrogen bonding were predicted between the phenol and the Arg119 side chain and Glu118 carbonyl backbone. Additionally, the 3-NH forms a hydrogen bond with the Glu116 carbonyl backbone. The thione moiety is oriented towards Ile136 deep within the binding pocket with the ethanoate group facing the water phase. The spatial orientation and intermolecular interactions are in agreement with X-ray crystallographic data reported by Garcia-Saez et al.[2] and molecular modelling studies on monastrol mimics by Soumyanarayanan et al.[3] The similarities in the docked configurations to the one described in the literature and a low RMSD value suggest the reliability and reproducibility of the docking protocol.

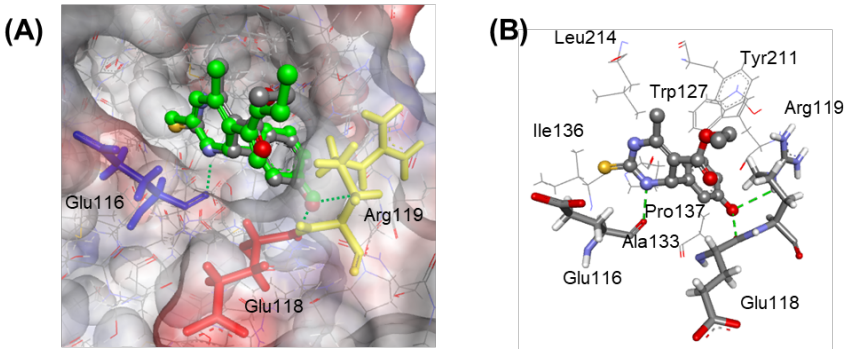

Supporting Figure S2. Docked configuration of (*S*)-monastrol. Hydrogen atoms have been omitted for clarity. H-bonds are depicted as green dotted lines. (A) Overlays between co-crystallized (*S*)-monastrol (green) and re-docked (*S*)-monastrol. Residues involved in hydrogen bonding; Glu116 (blue), Glu118 (red) and Arg119 (yellow) are shown. The surface of the allosteric site is rendered, hydrophobic, partial negative and postive regions are coloured grey, red and blue, respectively. (B) Docked configuration of (*S*)-monastrol surrounded by hydrophobic and hydrogen bonding amino acid residues.

^{1}H and $^{13}C\{^{1}H\}$ NMR spectra

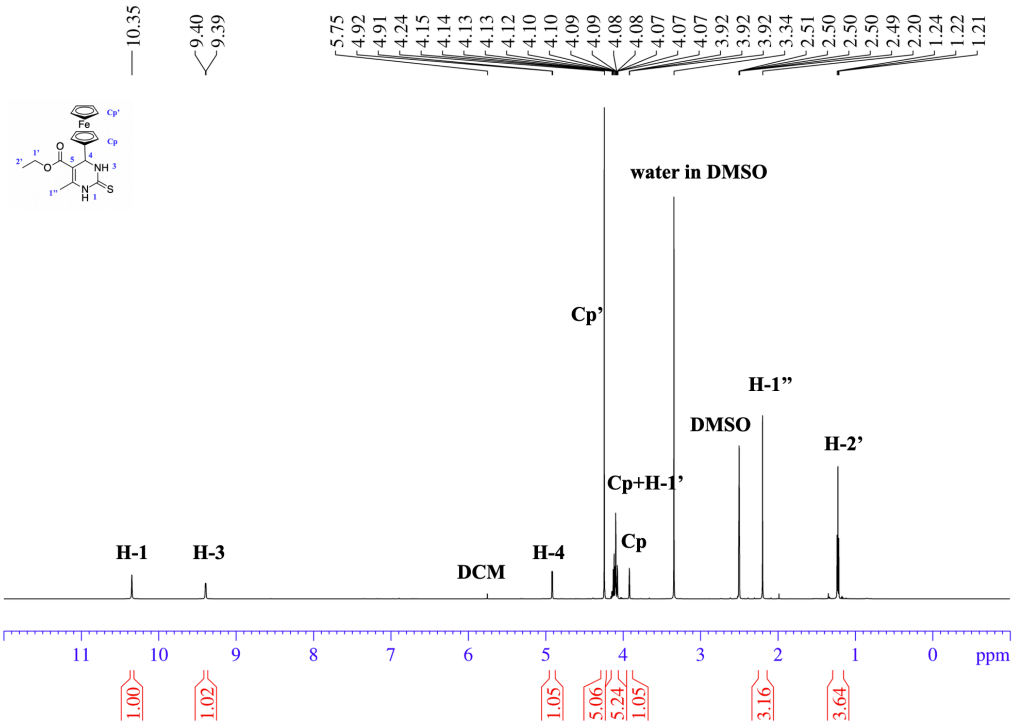

Supporting Figure S3. ^{1}H NMR spectra of 3a in DMSO-d_6.

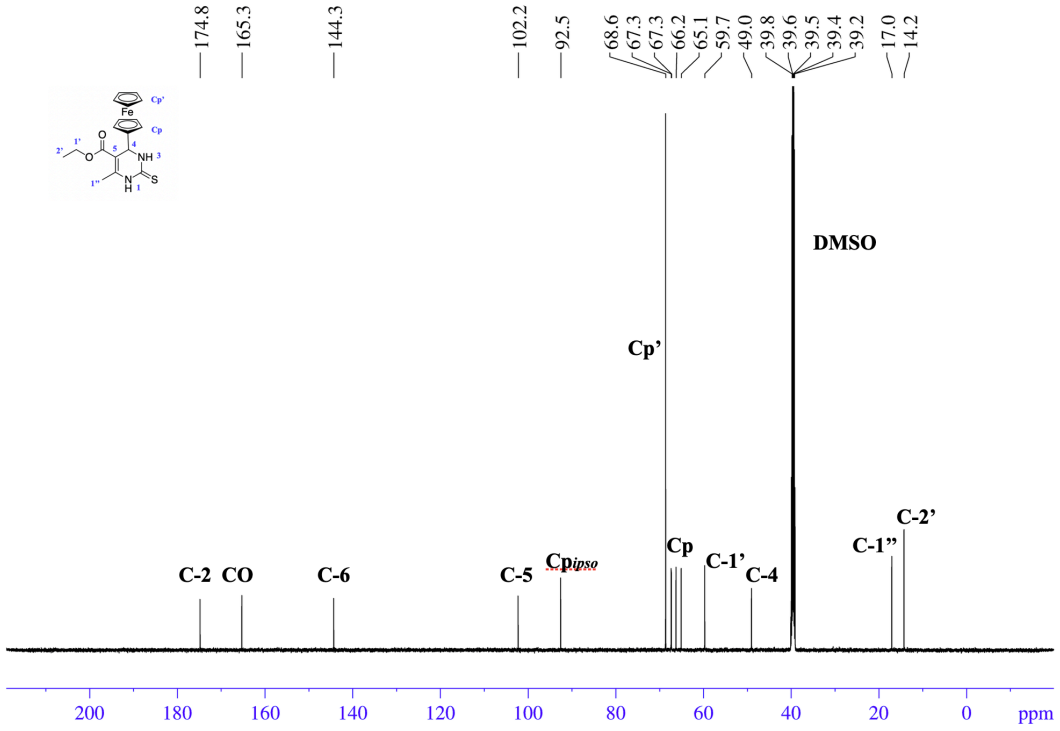

Supporting Figure S4. $^{13}C\{^{1}H\}$ NMR spectra of 3a in DMSO-d_6.

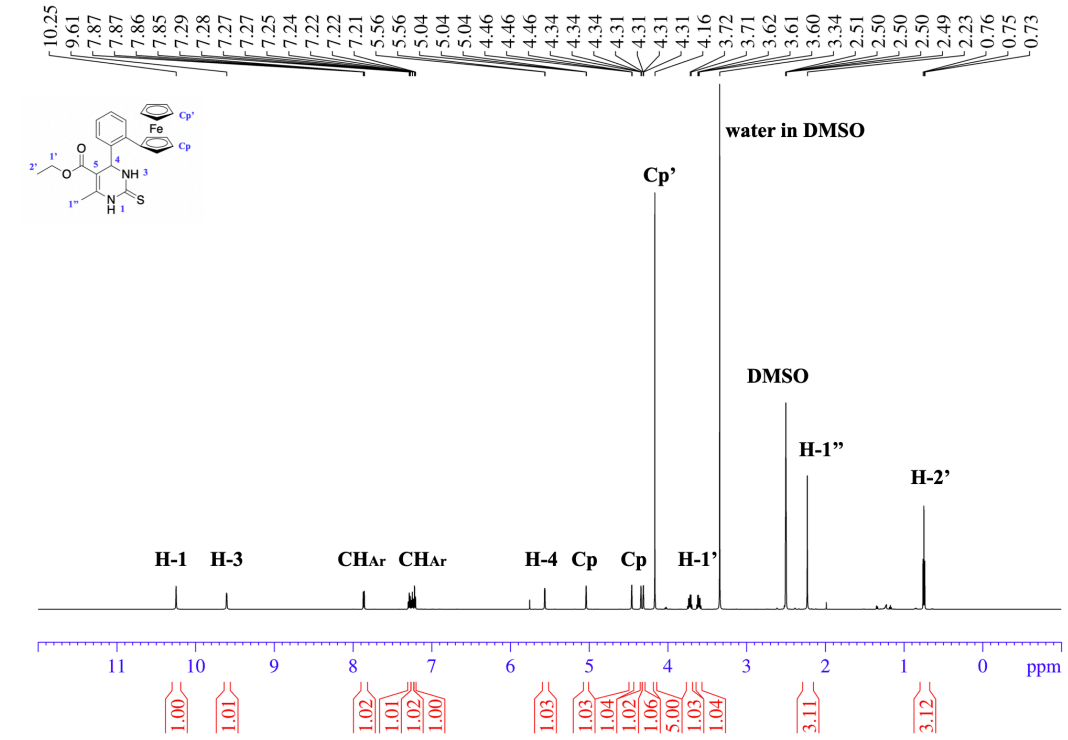

Supporting Figure S5. ^{1}H NMR spectra of 3b in DMSO-d$_6$.

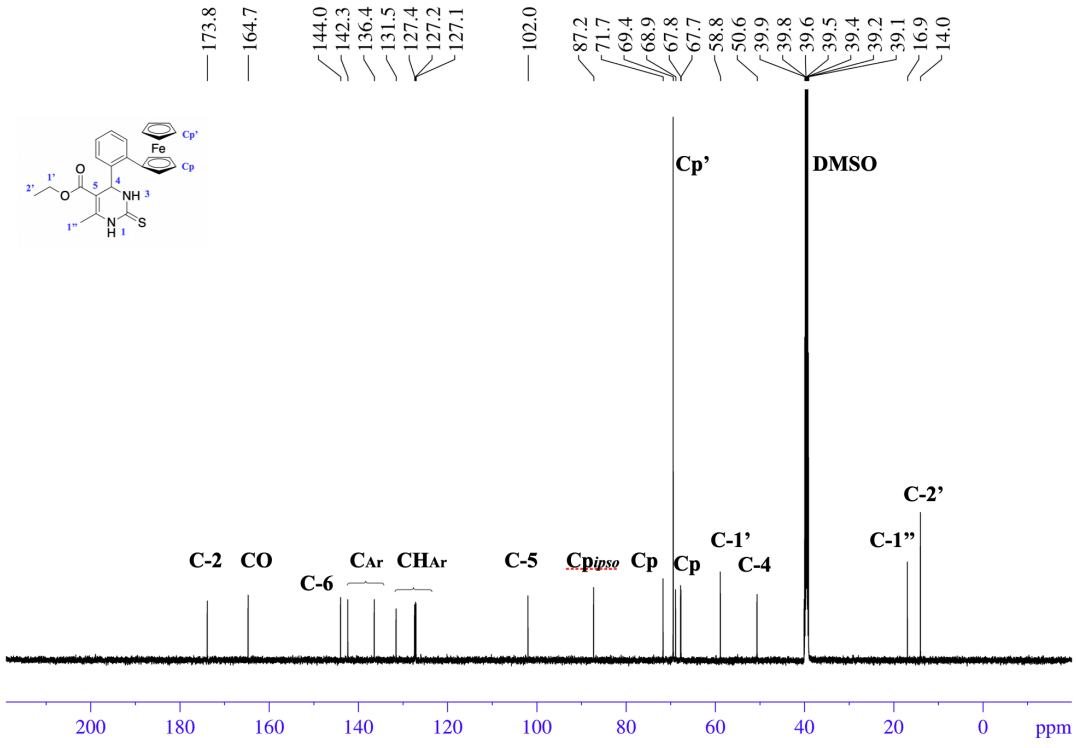

Supporting Figure S6. ^{13}C{^{1}H} NMR spectra of 3b in DMSO-d$_6$.

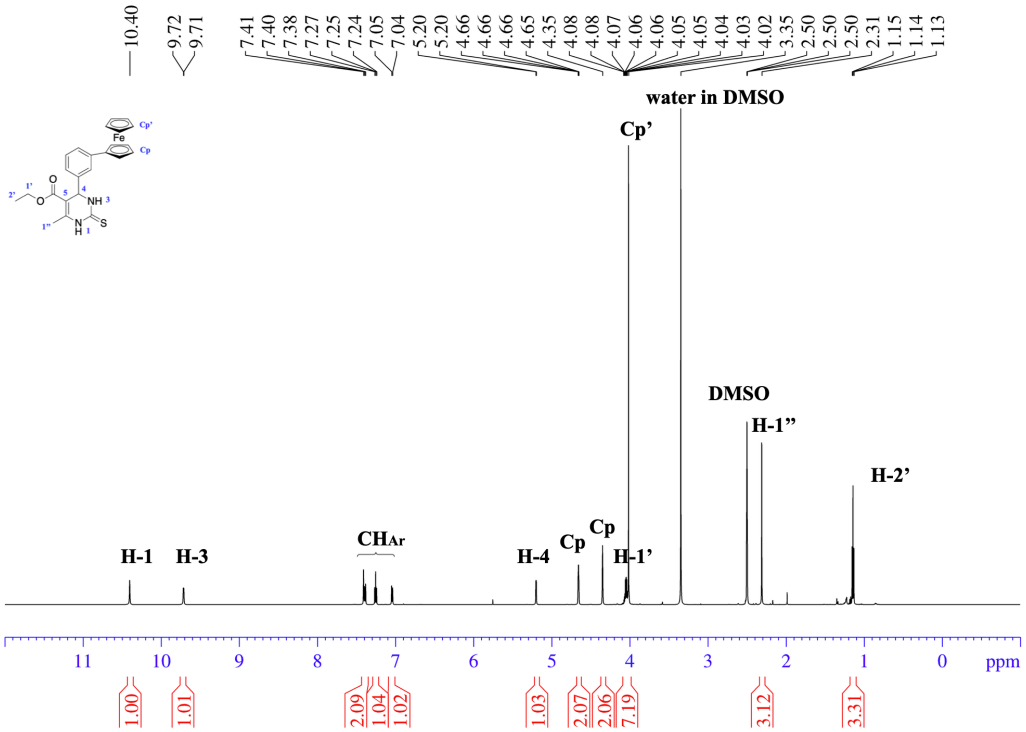

Supporting Figure S7. ^{1}H NMR spectra of 3c in DMSO-d_6.

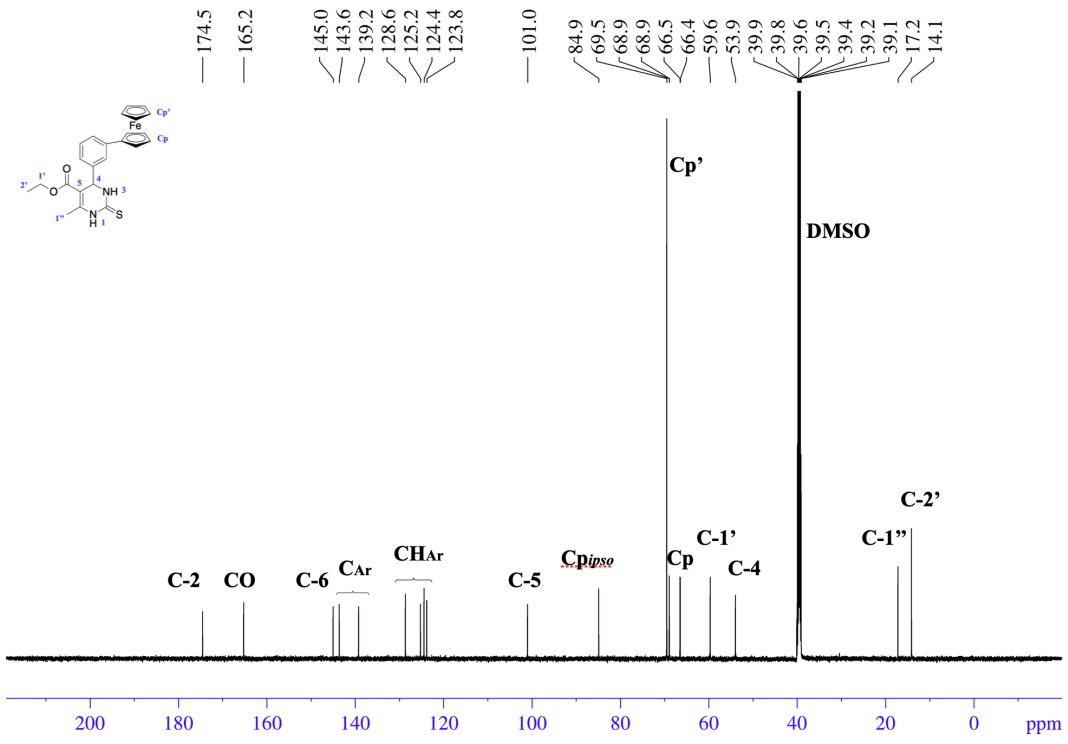

Supporting Figure S8. $^{13}C\{^{1}H\}$ NMR spectra of 3c in DMSO-d_6.

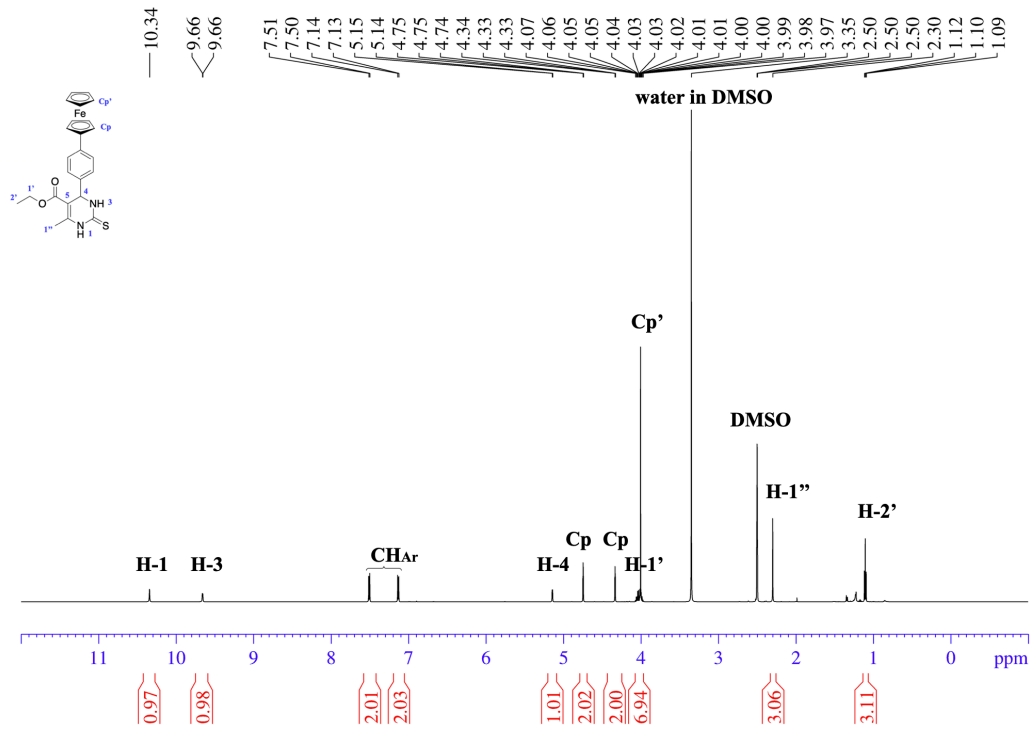

Supporting Figure S9. ^{1}H NMR spectra of 3d in DMSO-d$_6$.

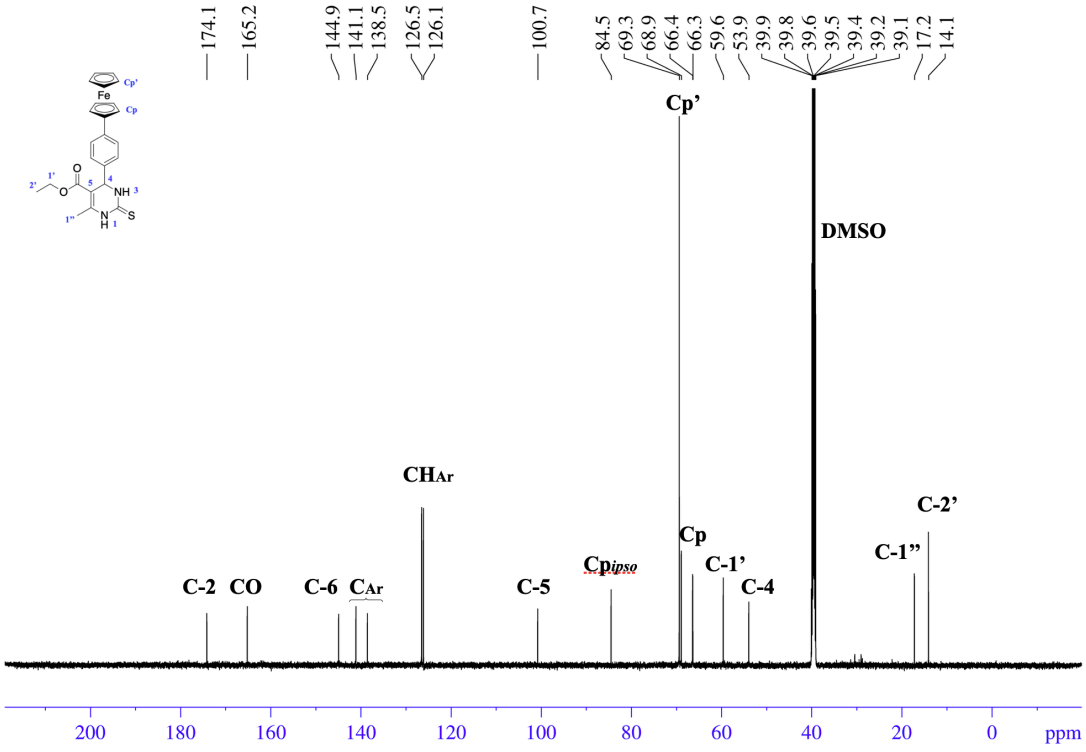

Supporting Figure S10. ^{13}C{^{1}H} NMR spectra of 3d in DMSO-d$_6$.

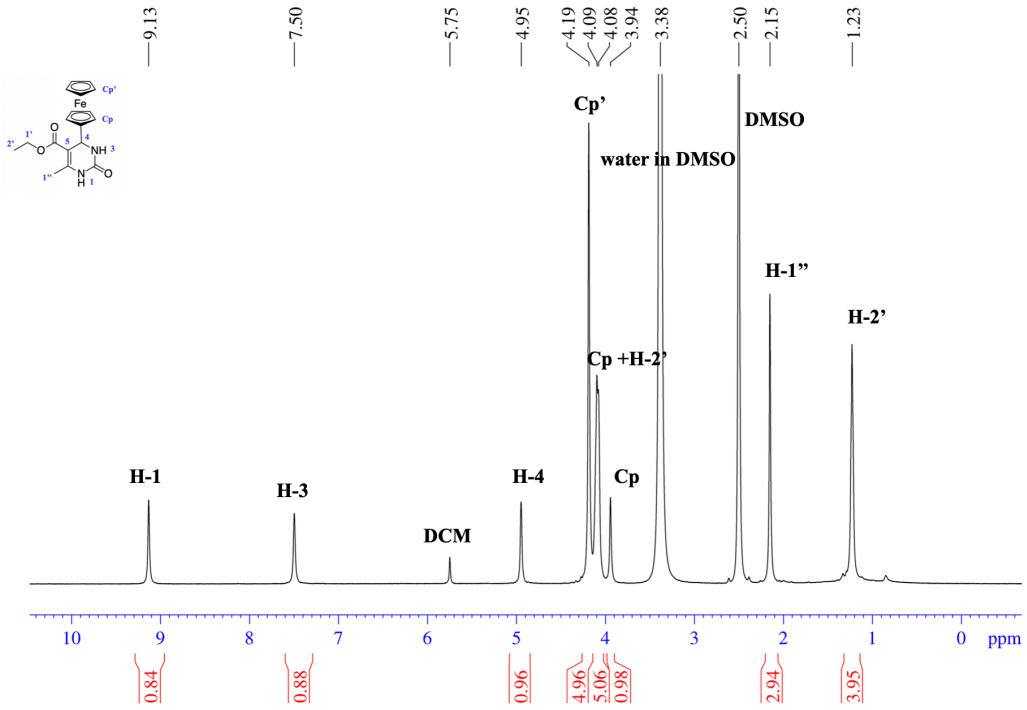

Supporting Figure S11. ^{1}H NMR spectra of 4a in DMSO-d$_6$.

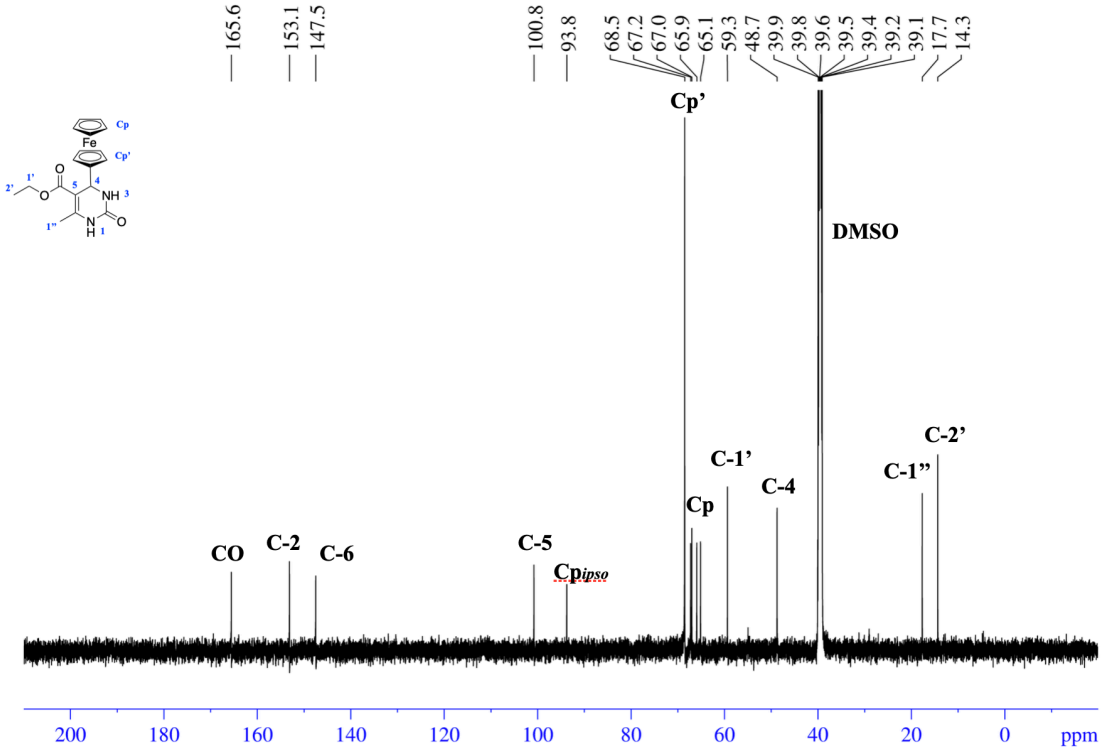

Supporting Figure S12. ^{13}C{^{1}H} NMR spectra of 4a in DMSO-d$_6$.

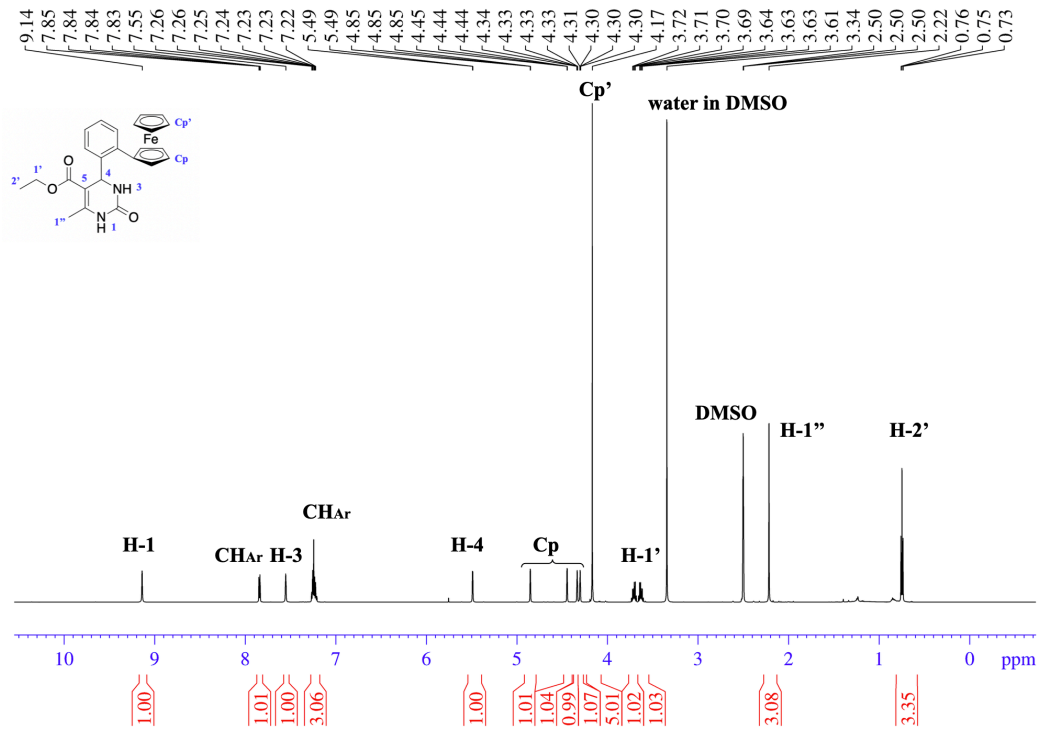

Supporting Figure S13. ^{1}H NMR spectra of 4b in DMSO-d$_6$.

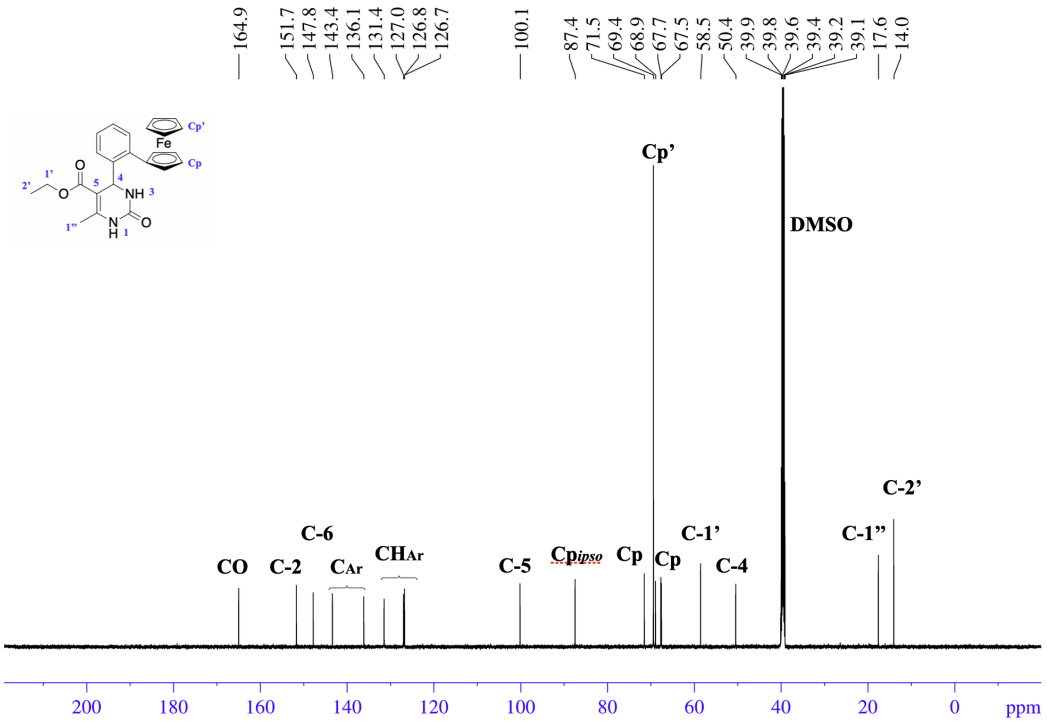

Supporting Figure S14. ^{13}C{^{1}H} NMR spectra of 4b in DMSO-d$_6$.

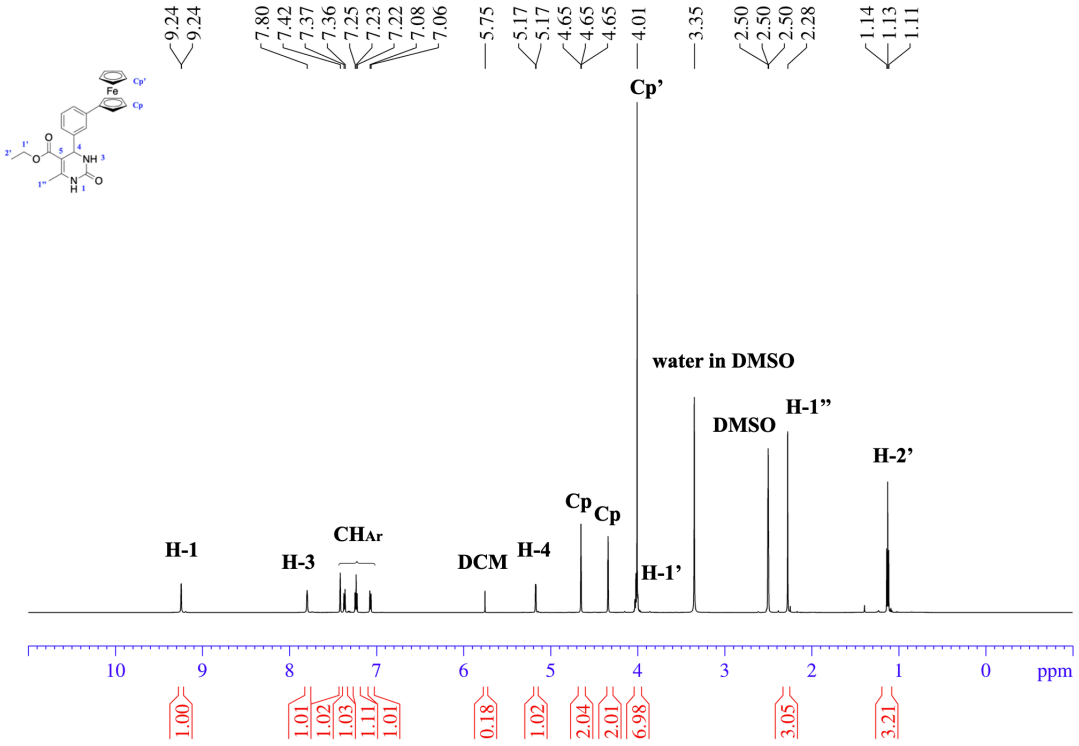

Supporting Figure S15. ^{1}H NMR spectra of 4c in DMSO-d$_6$.

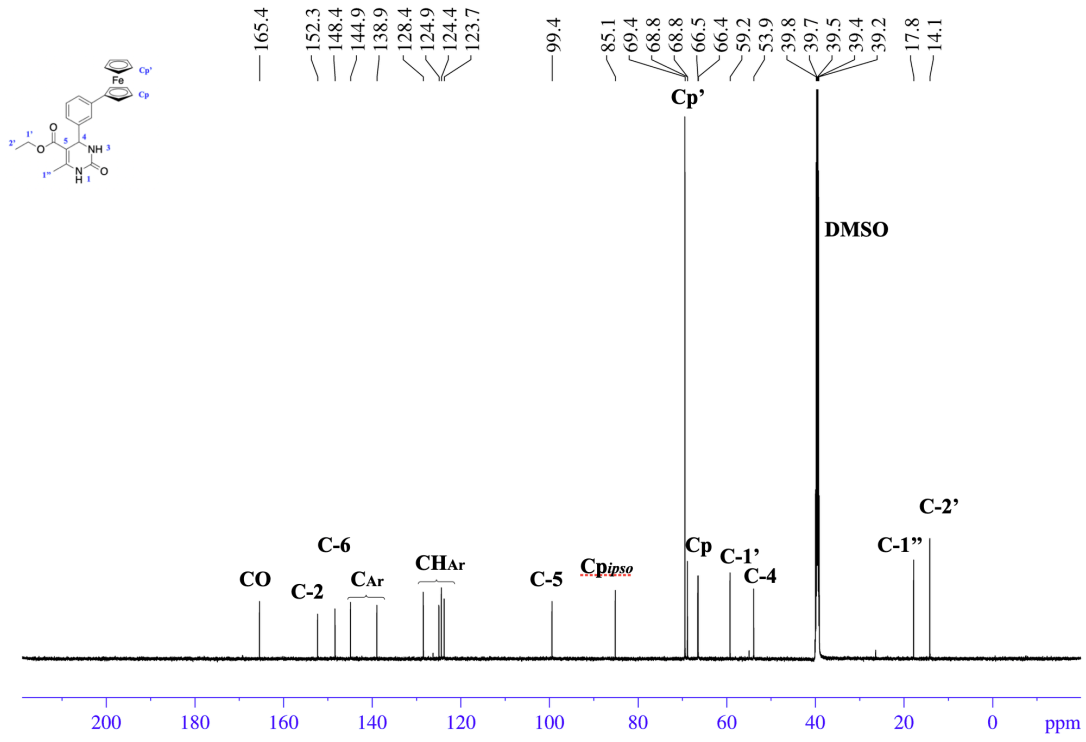

Supporting Figure S16. ^{13}C{^{1}H} NMR spectra of 4c in DMSO-d$_6$.

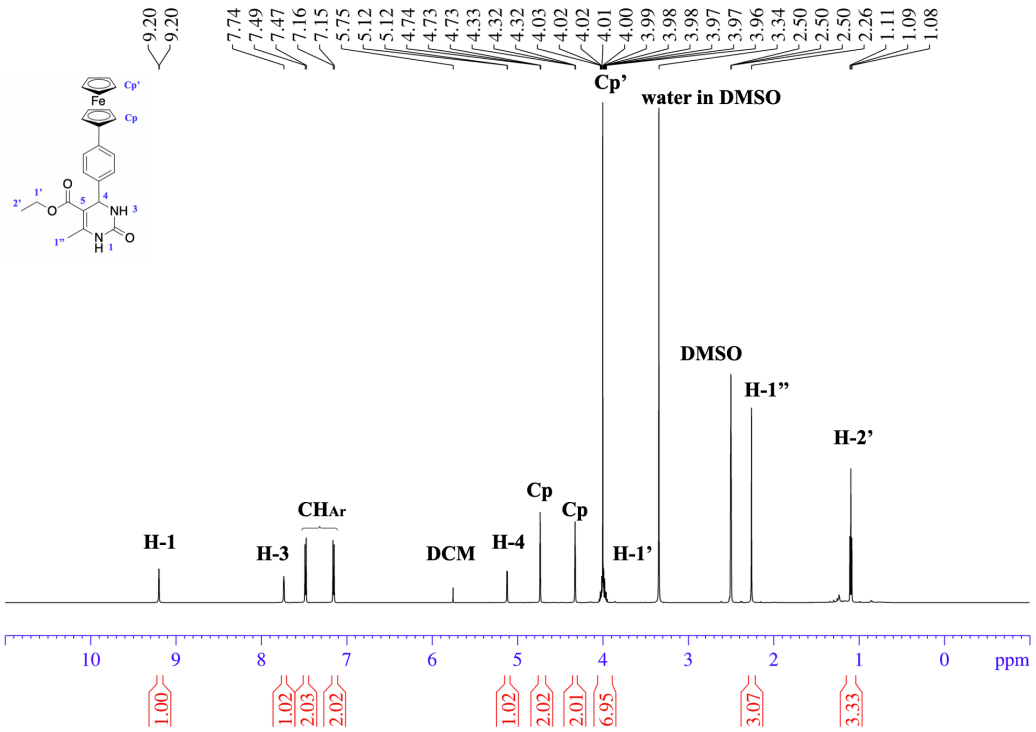

Supporting Figure S17. ^{1}H NMR spectra of 4d in DMSO-d$_6$.

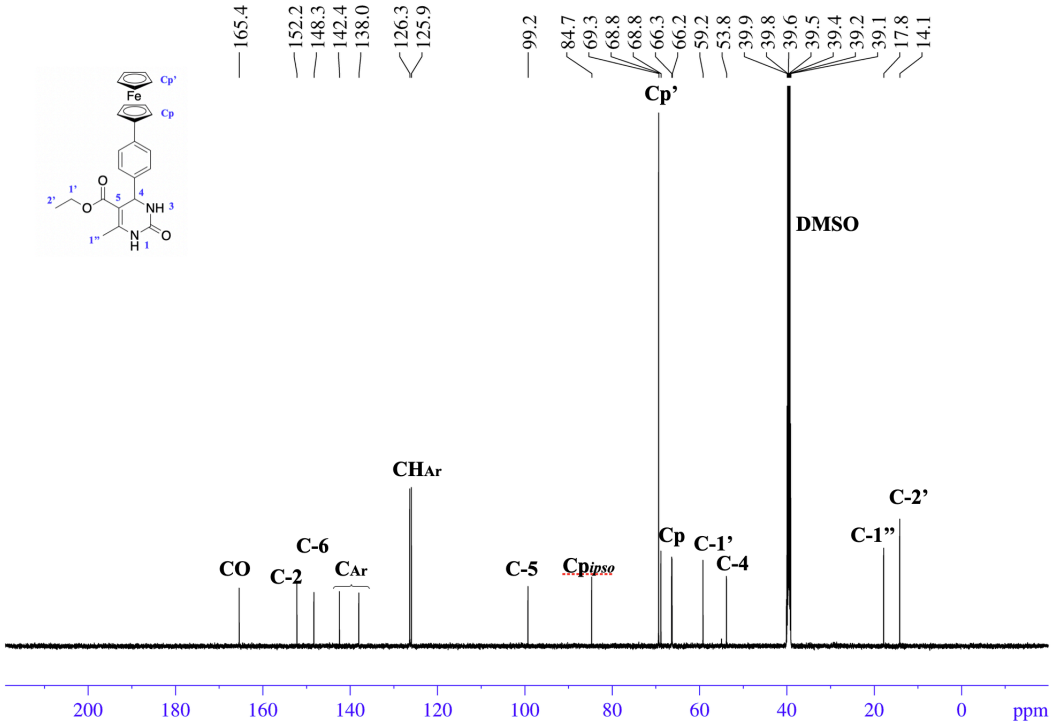

Supporting Figure S18. ^{13}C{^{1}H} NMR spectra of 4d in DMSO-d$_6$.

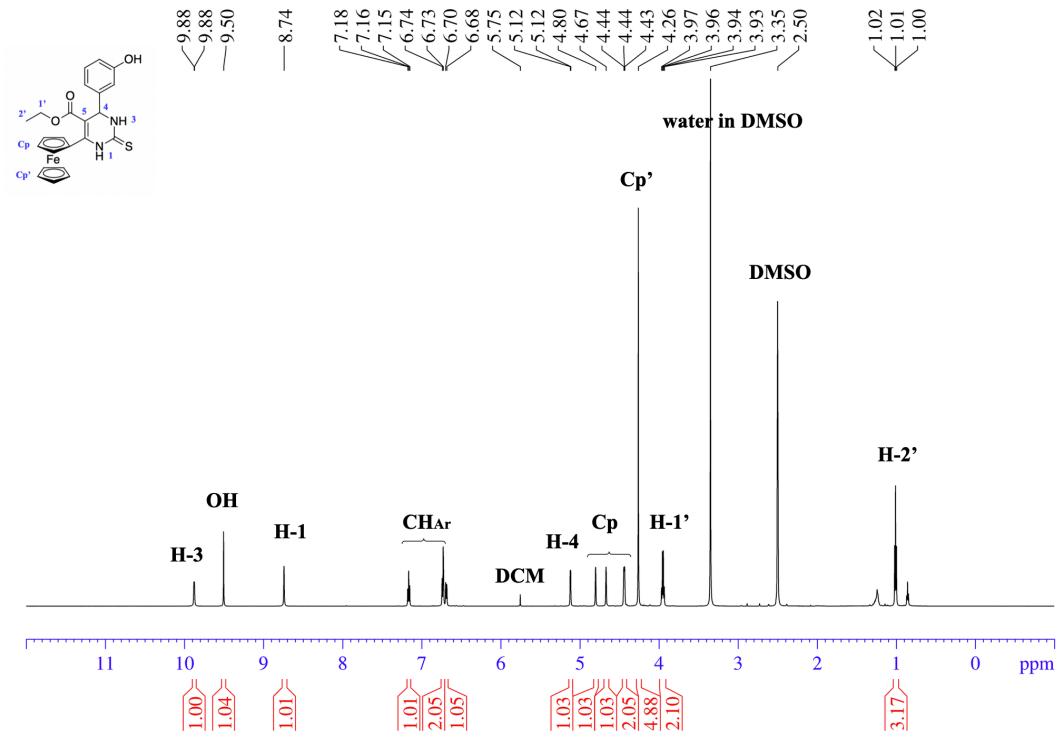

Supporting Figure S19. ^{1}H NMR spectra of 6a in DMSO-d$_6$.

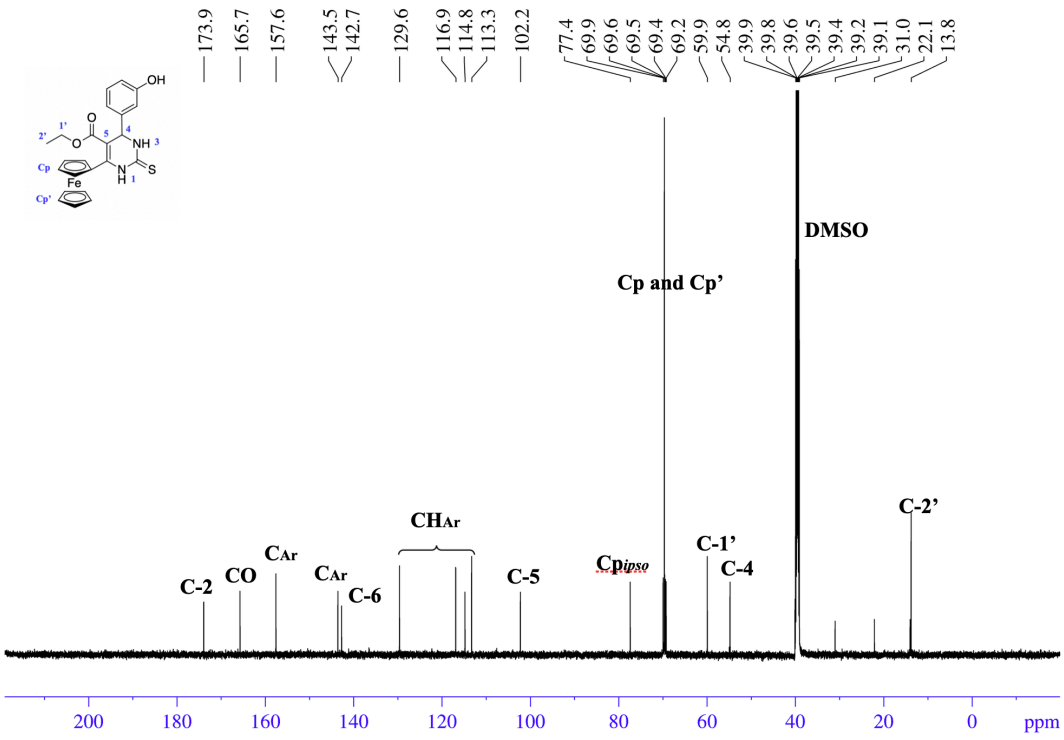

Supporting Figure S20. ^{13}C{^{1}H} NMR spectra of 6a in DMSO-d$_6$.

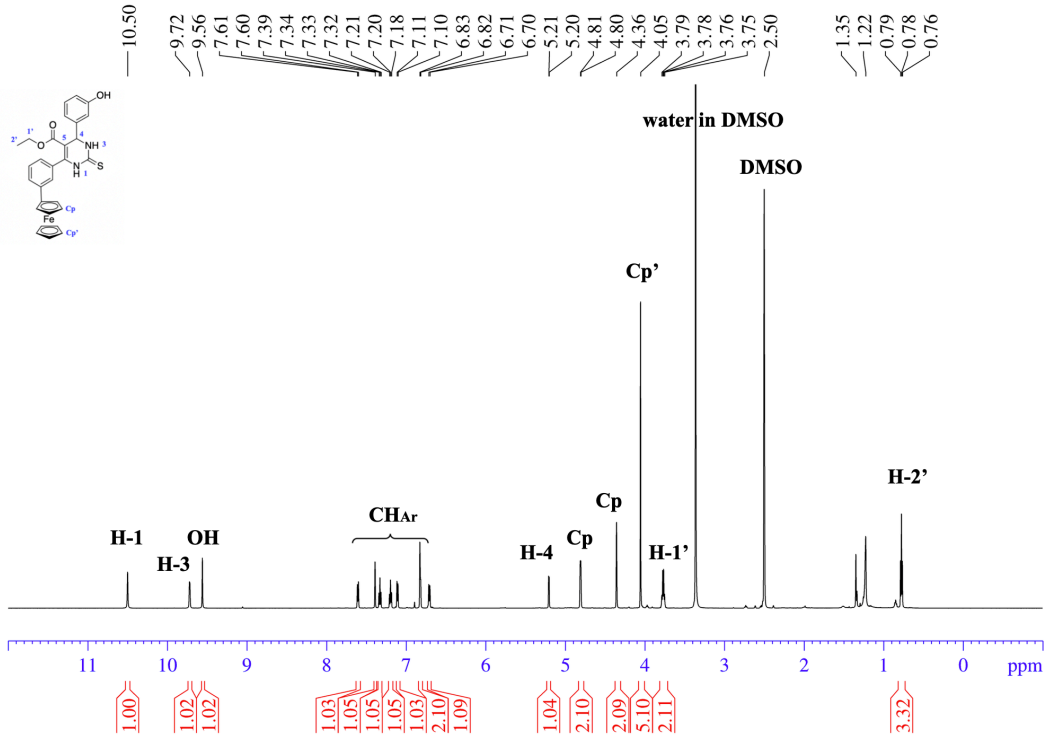

Supporting Figure S21. ^{1}H NMR spectra of 6c in DMSO-d$_6$.

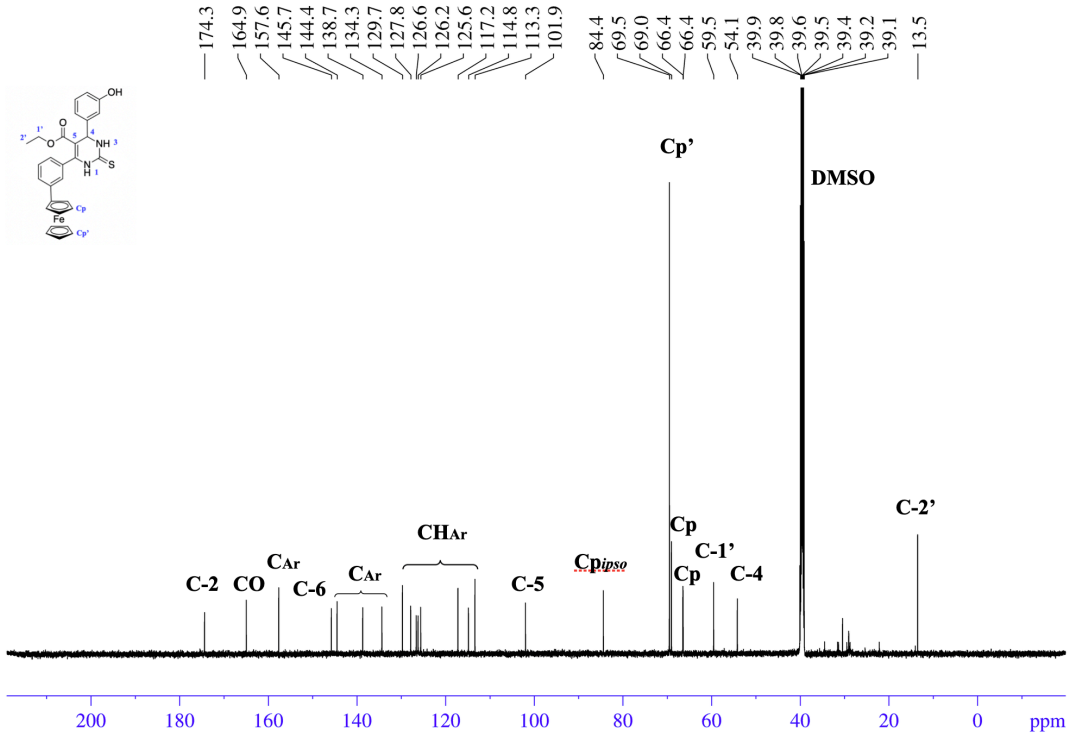

Supporting Figure S22. ^{13}C{^{1}H} NMR spectra of 6c in DMSO-d$_6$.

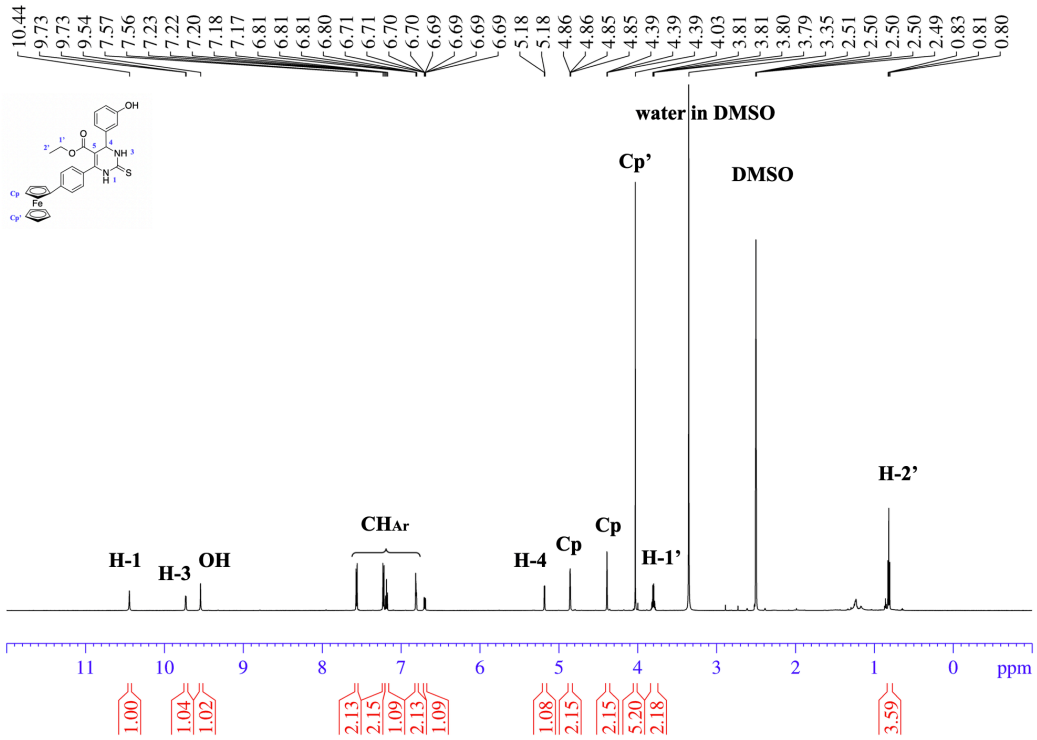

Supporting Figure S23. ^{1}H NMR spectra of 6d in DMSO-d$_6$.

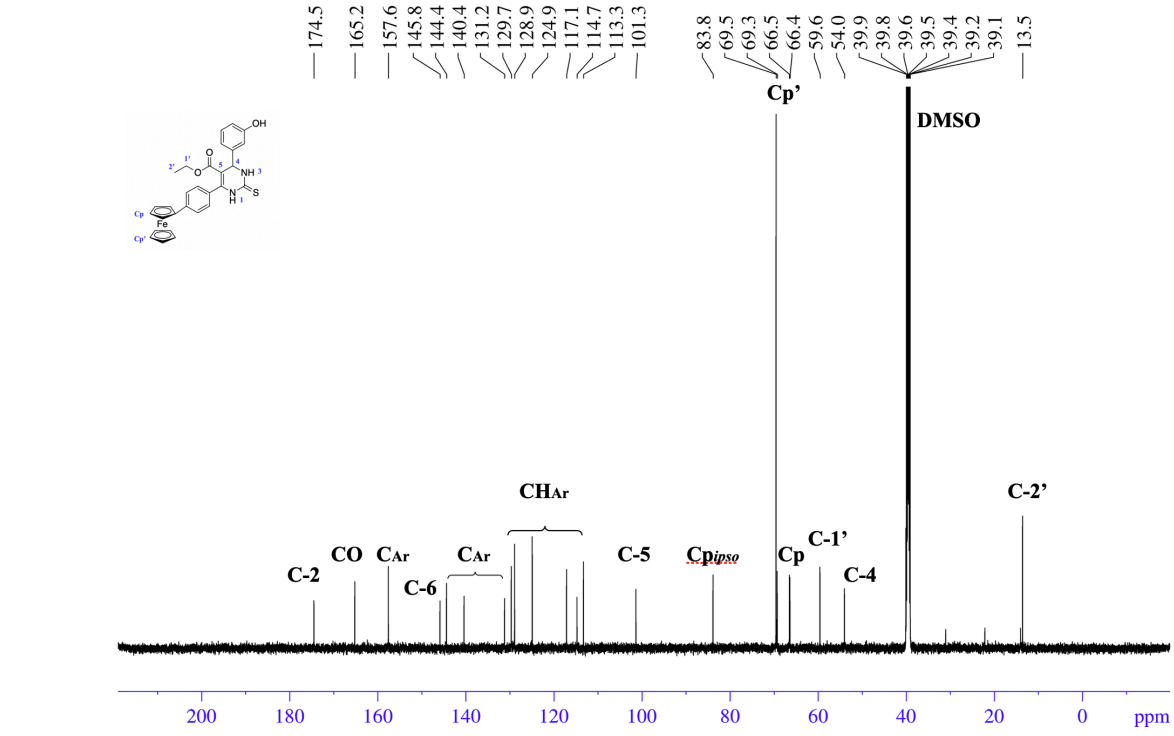

Supporting Figure S24. ^{13}C{^{1}H} NMR spectra of 6d in DMSO-d$_6$.

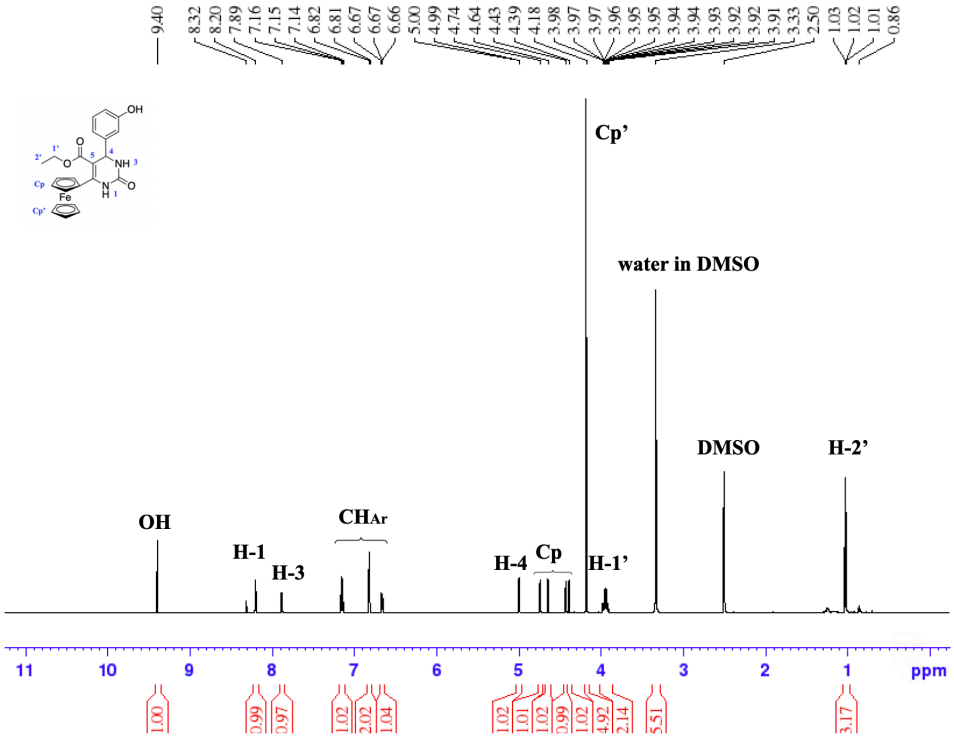

Supporting Figure S25. ^{1}H NMR spectra of 7a in DMSO-d$_6$.

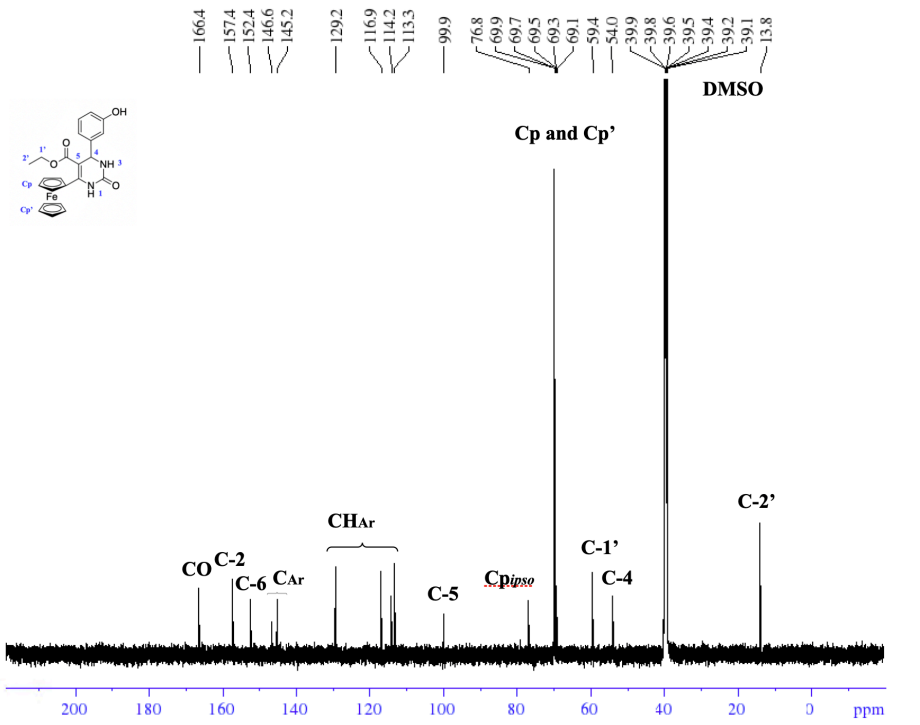

Supporting Figure S26. ^{13}C{^{1}H} NMR spectra of 7a in DMSO-d$_6$.

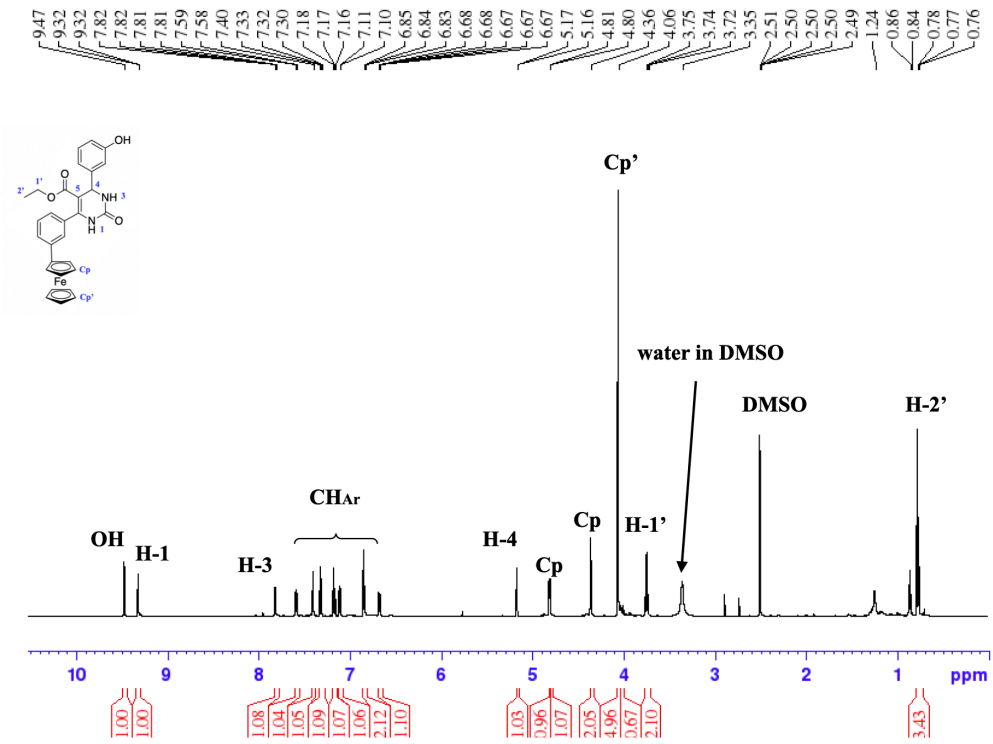

Supporting Figure S27. ^{1}H NMR spectra of 7c in DMSO-d$_6$.

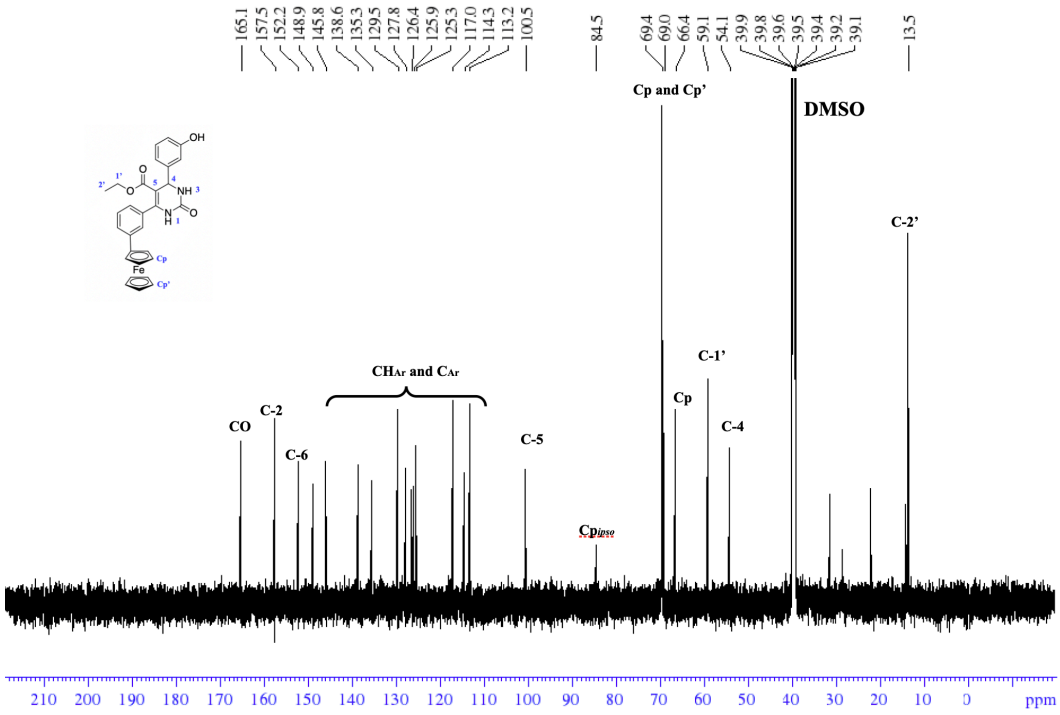

Supporting Figure S28. ^{13}C{^{1}H} NMR spectra of 7c in DMSO-d$_6$.

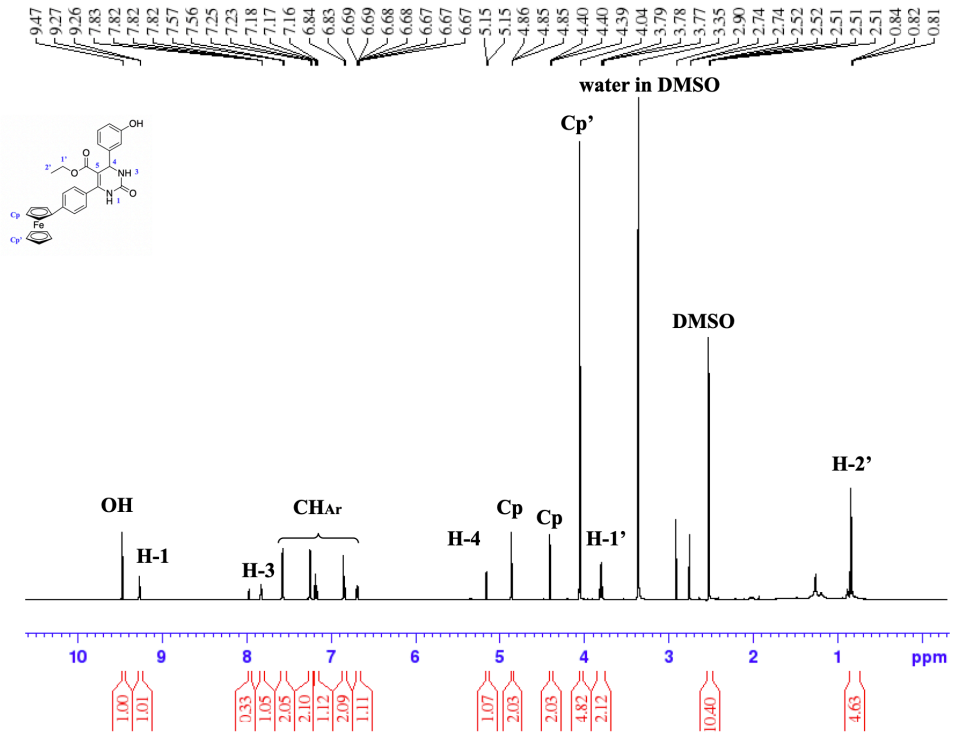

Supporting Figure S29. ^{1}H NMR spectra of 7d in DMSO-d$_6$.

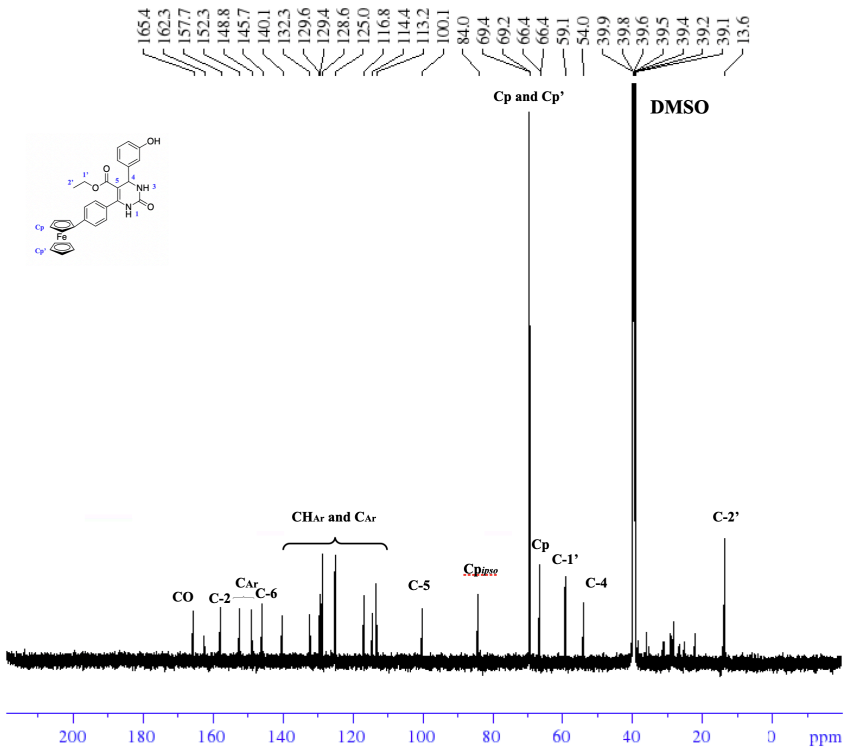

Supporting Figure S30. ^{13}C{^{1}H} NMR spectra of 7d in DMSO-d$_6$.

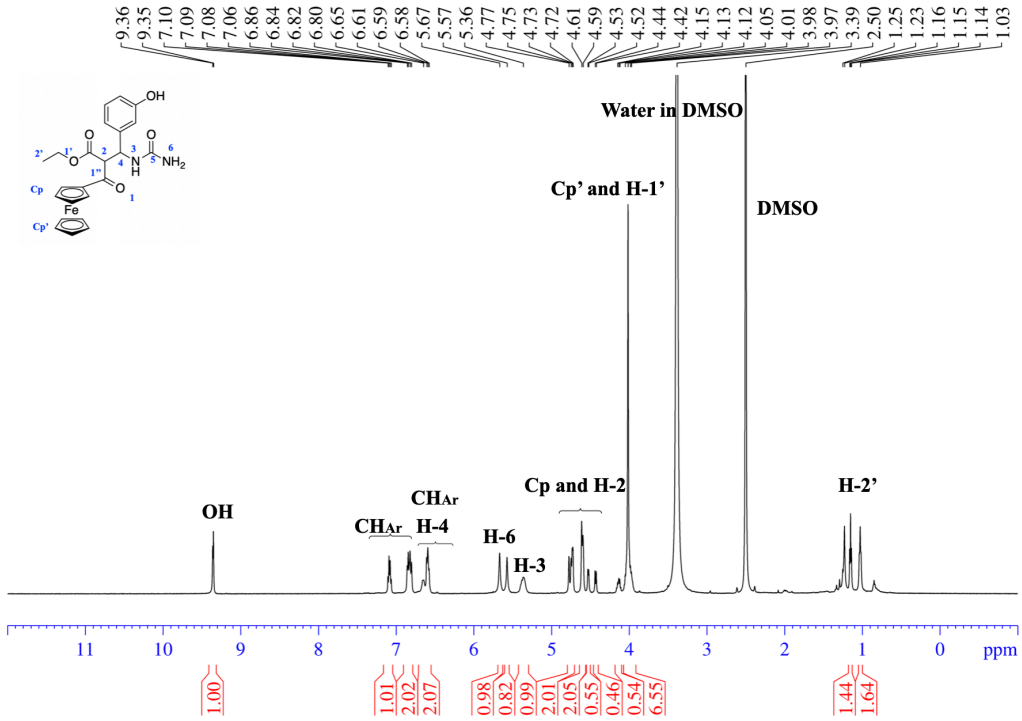

Supporting Figure S31. ^{1}H NMR spectra of 8a in DMSO-d$_6$.

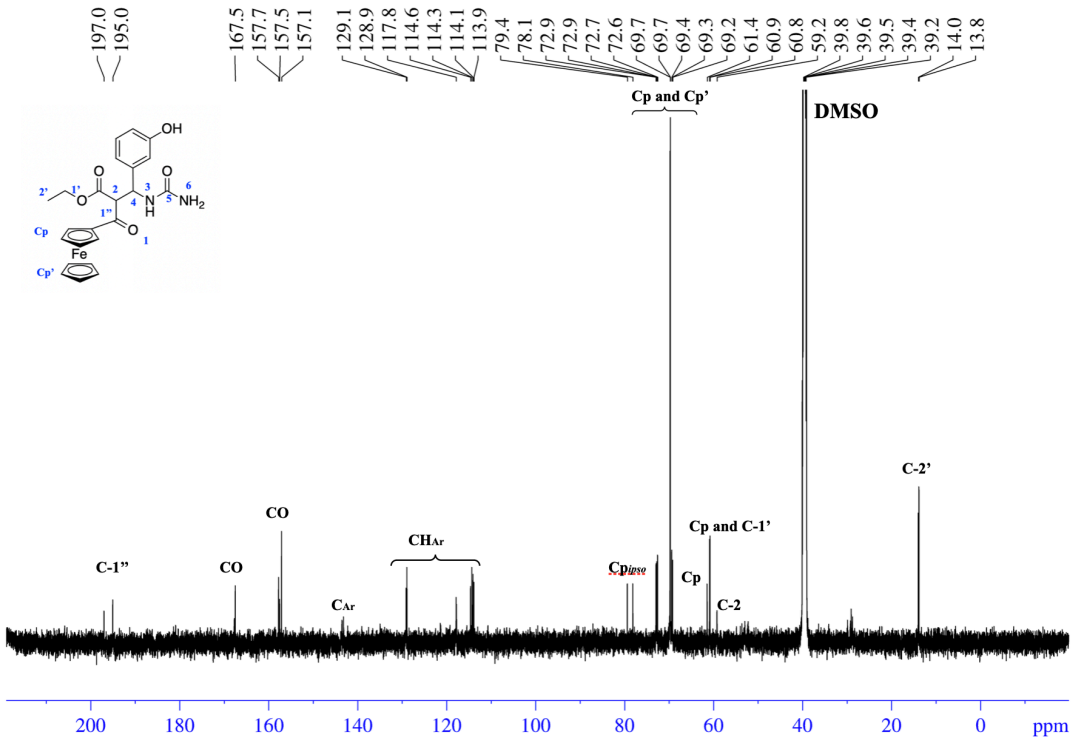

Supporting Figure S32. ^{13}C{^{1}H} NMR spectra of 8a in DMSO-d$_6$.

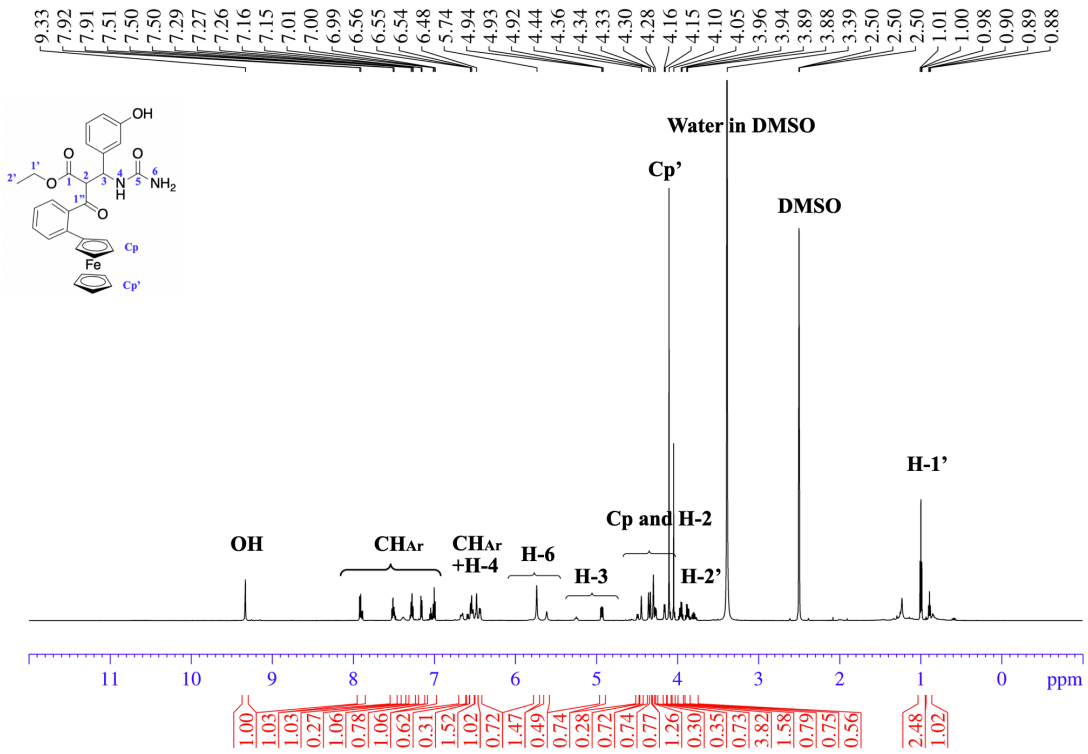

Supporting Figure S33. ^{1}H NMR spectra of 8b in DMSO-d$_6$.

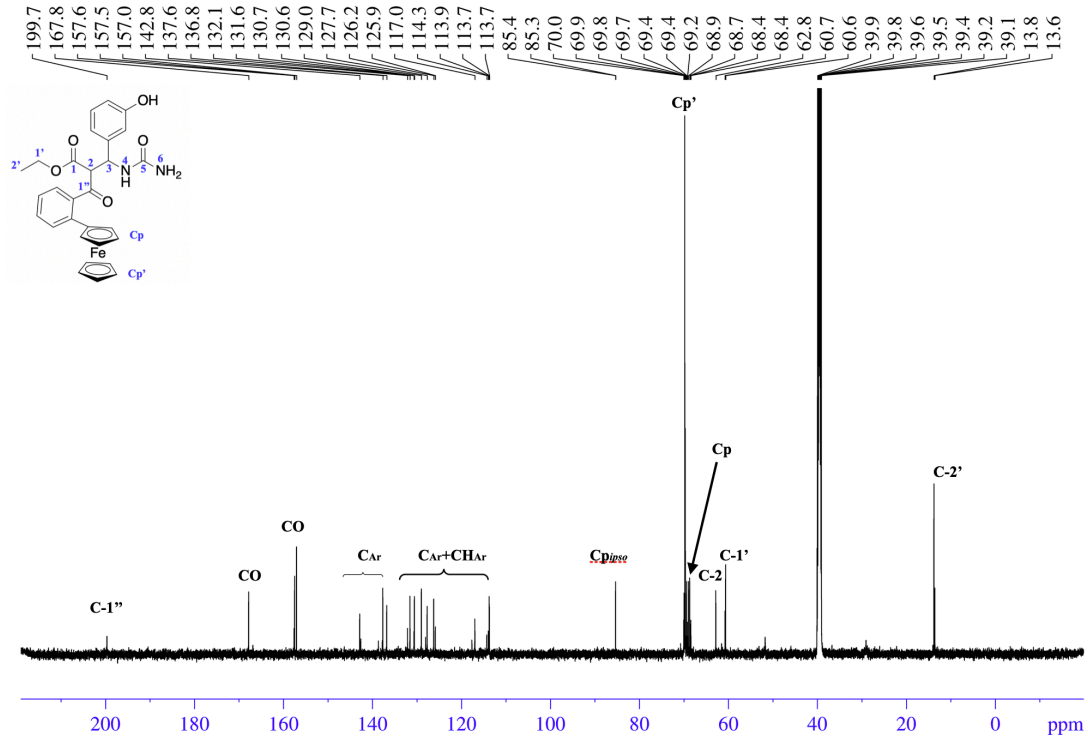

Supporting Figure S34. ^{13}C{^{1}H} NMR spectra of 8b in DMSO-d$_6$.

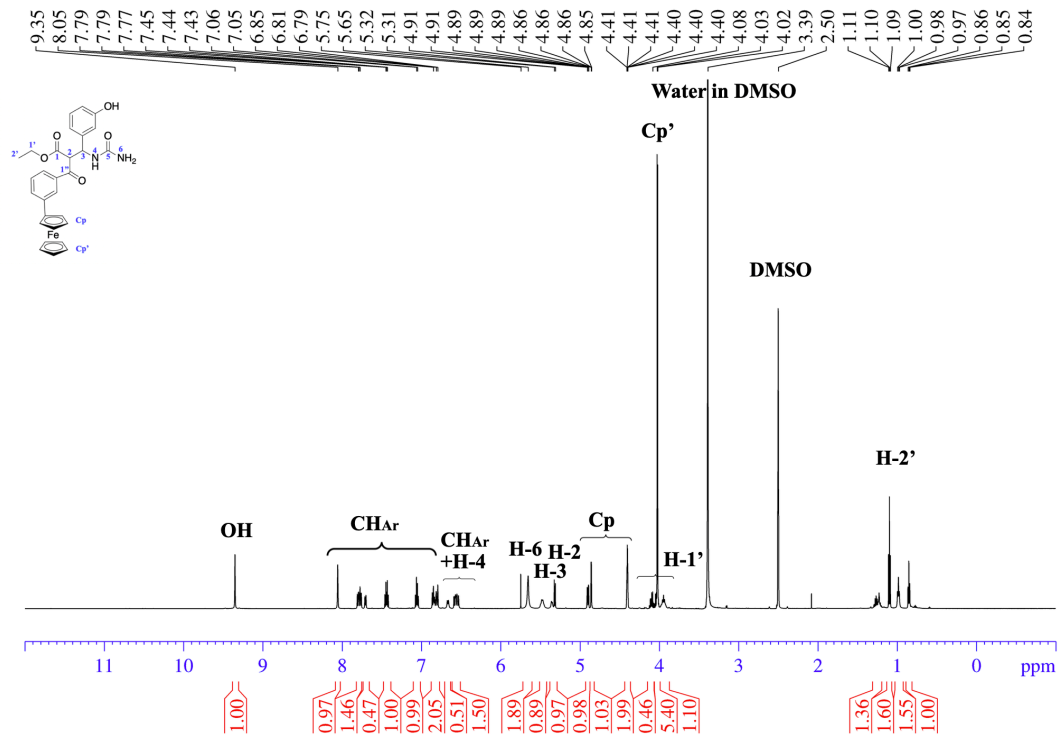

Supporting Figure S35. ^{1}H NMR spectra of 8c in DMSO-d$_6$.

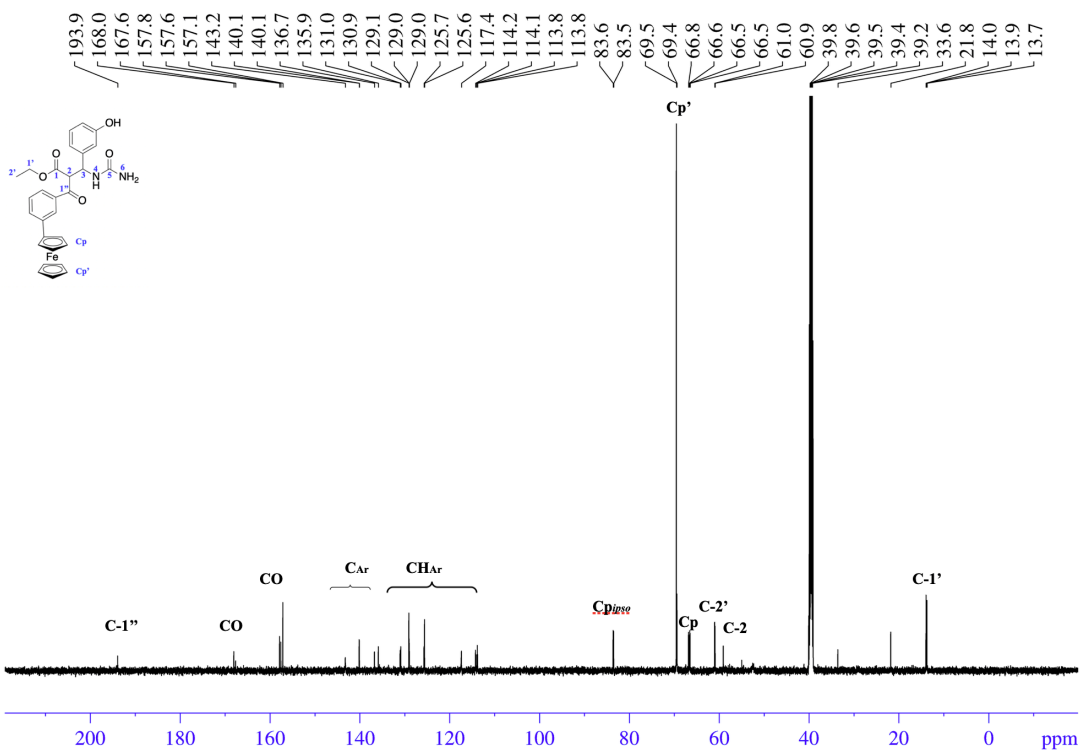

Supporting Figure S36. ^{13}C{^{1}H} NMR spectra of 8c in DMSO-d$_6$.

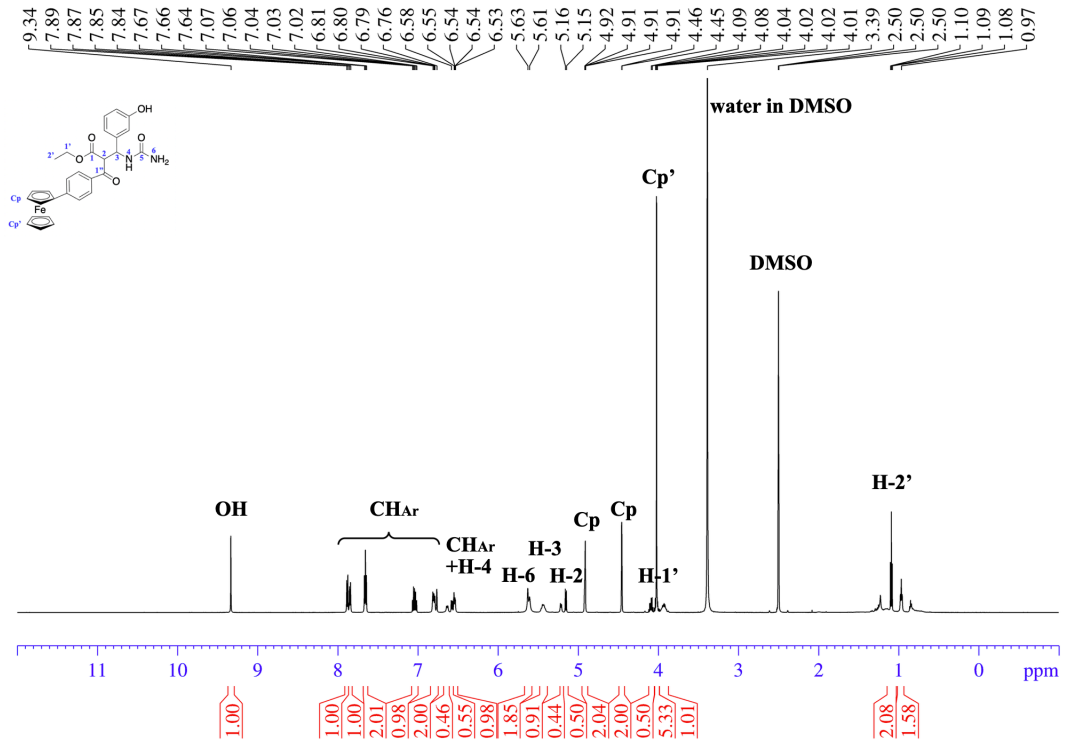

Supporting Figure S37. ^{1}H NMR spectra of 8d in DMSO-d$_6$.

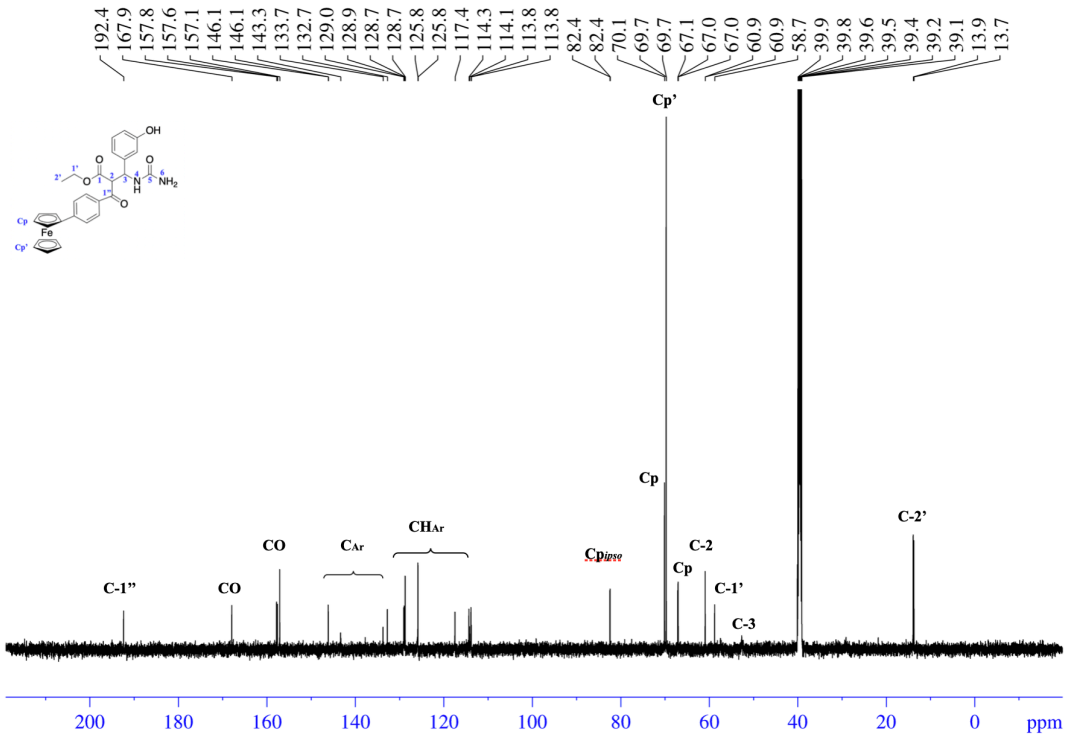

Supporting Figure S38. ^{13}C{^{1}H} NMR spectra of 8d in DMSO-d$_6$.

LC-MS analysis

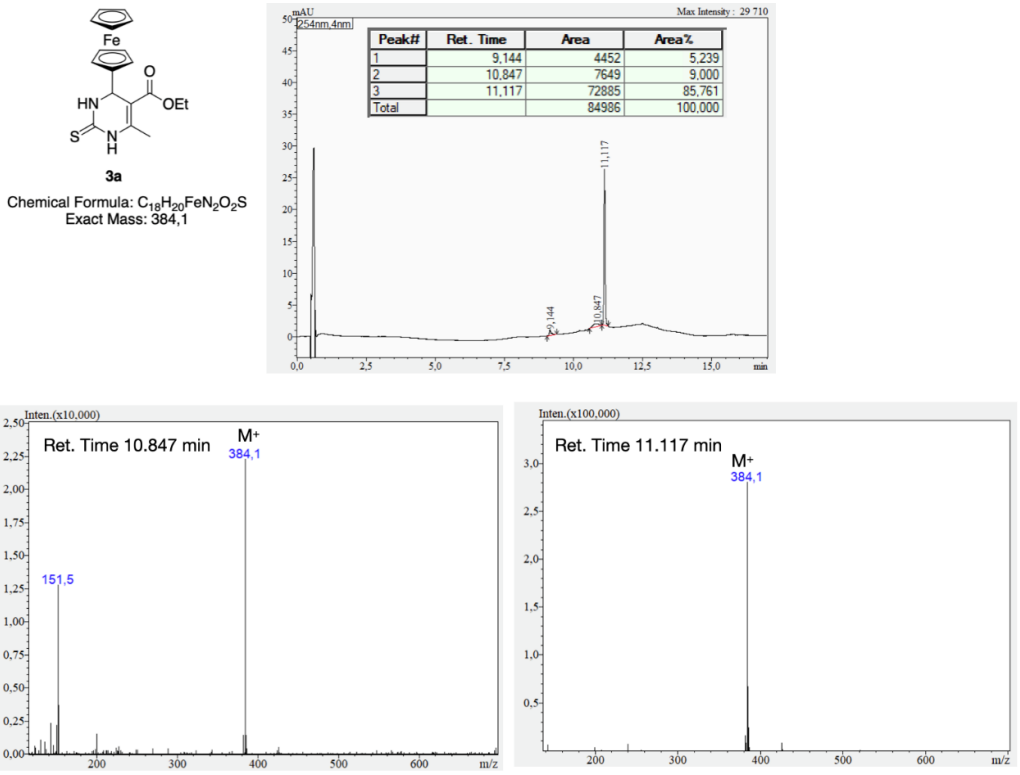

Supporting Figure S39. LC-MS analysis of 3a.

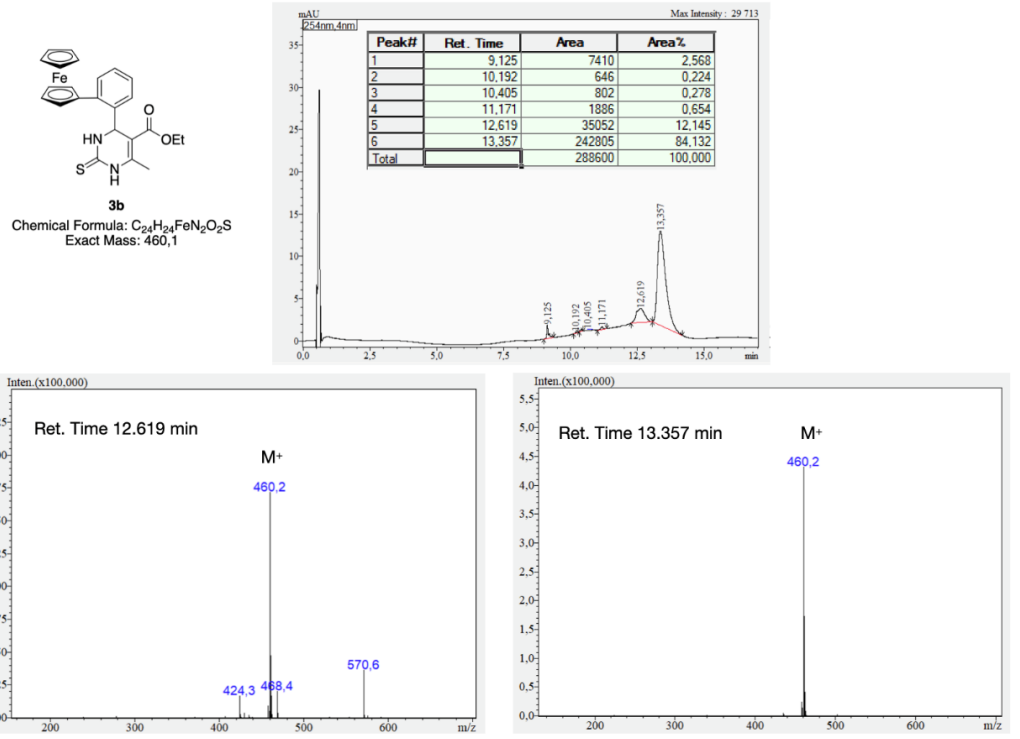

Supporting Figure S40. LC-MS analysis of 3b.

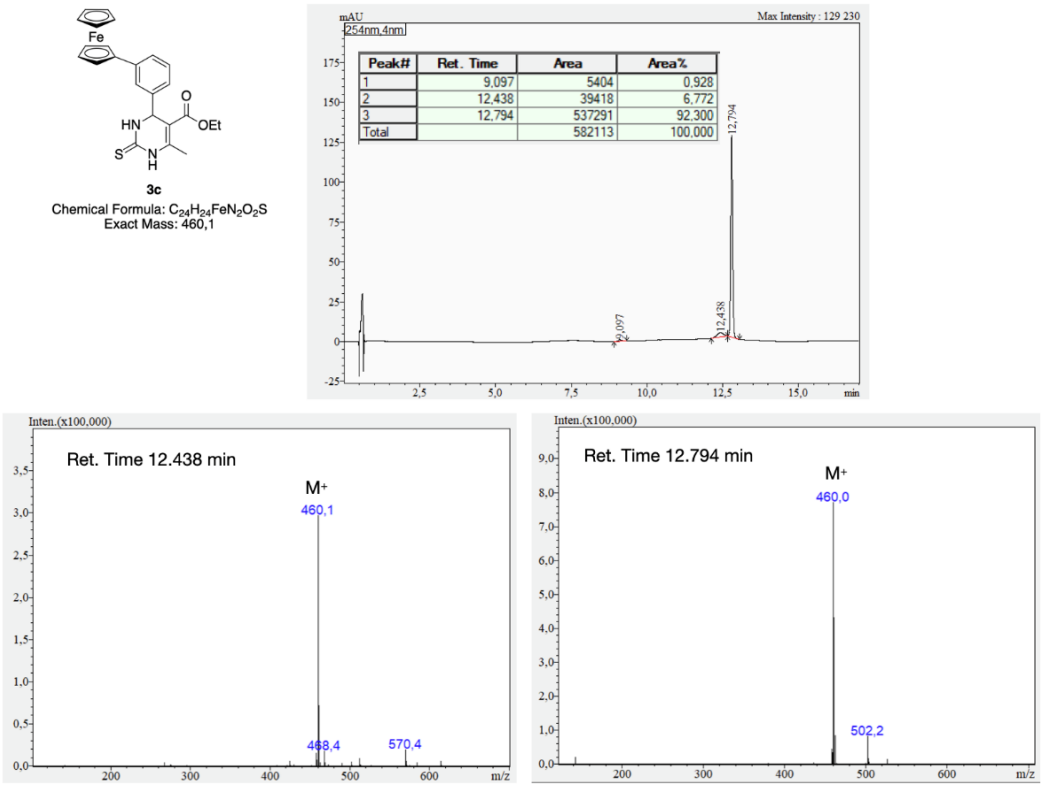

Supporting Figure S41. LC-MS analysis of 3c.

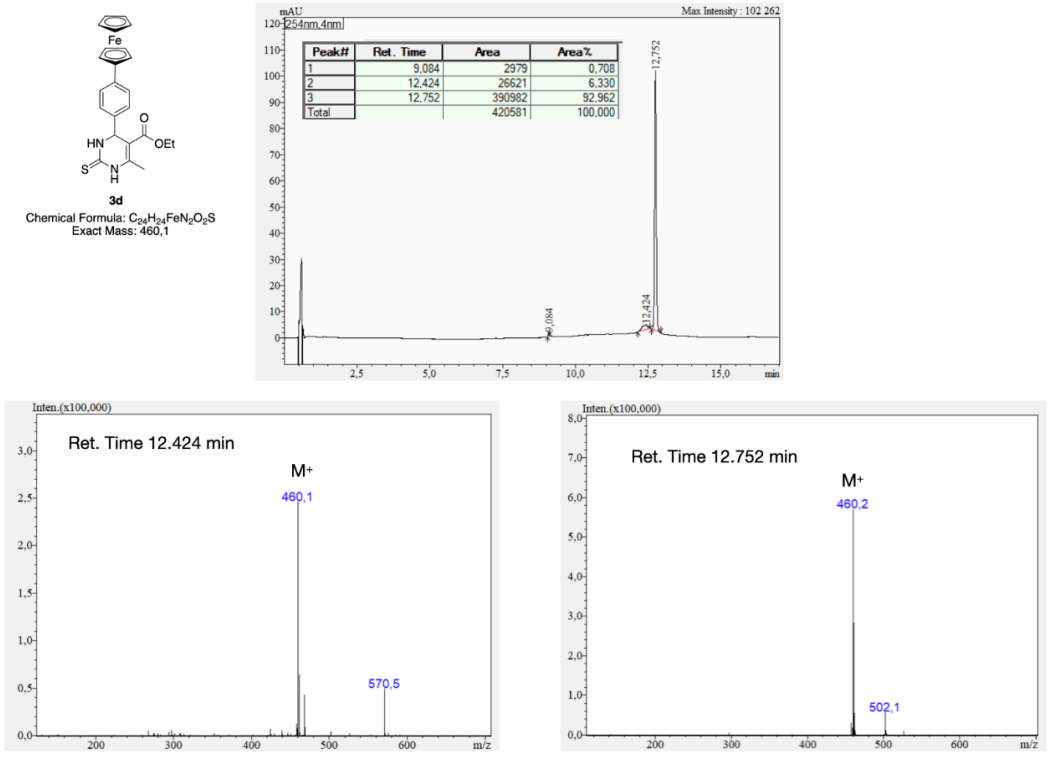

Supporting Figure S42. LC-MS analysis of 3d.

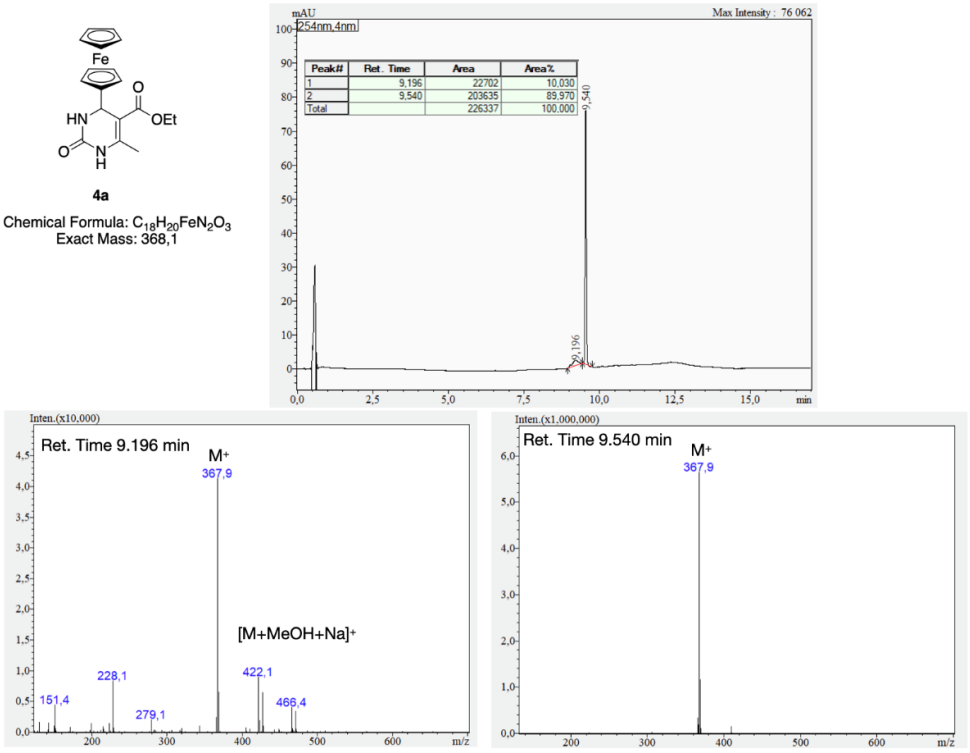

Supporting Figure S43. LC-MS analysis of 4a.

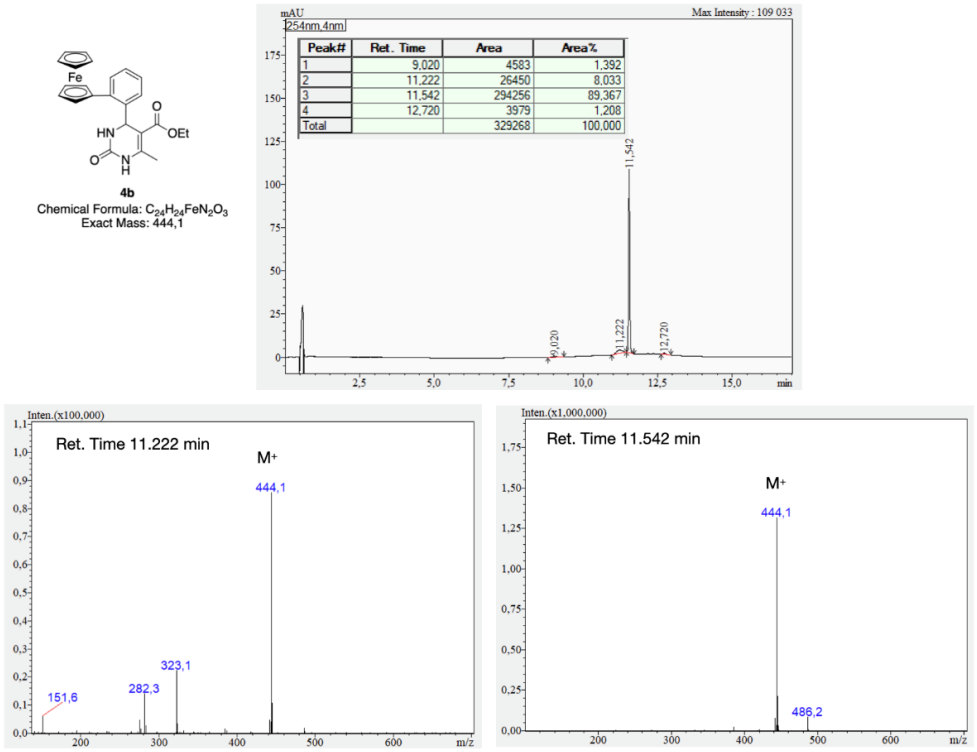

Supporting Figure S44. LC-MS analysis of 4b.

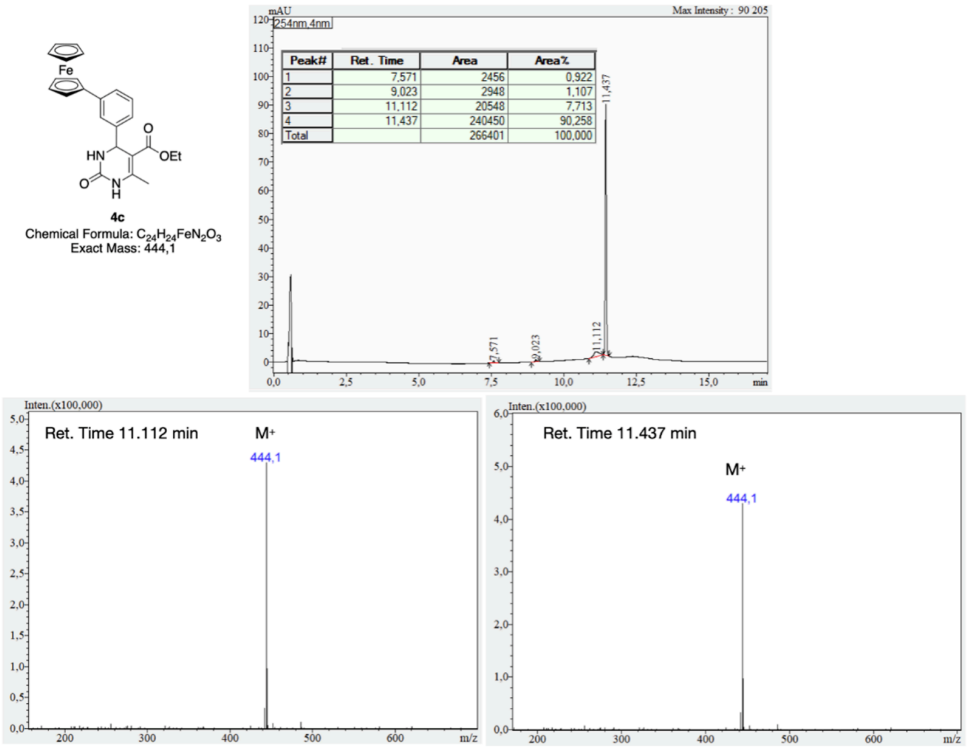

Supporting Figure S45. LC-MS analysis of 4c.

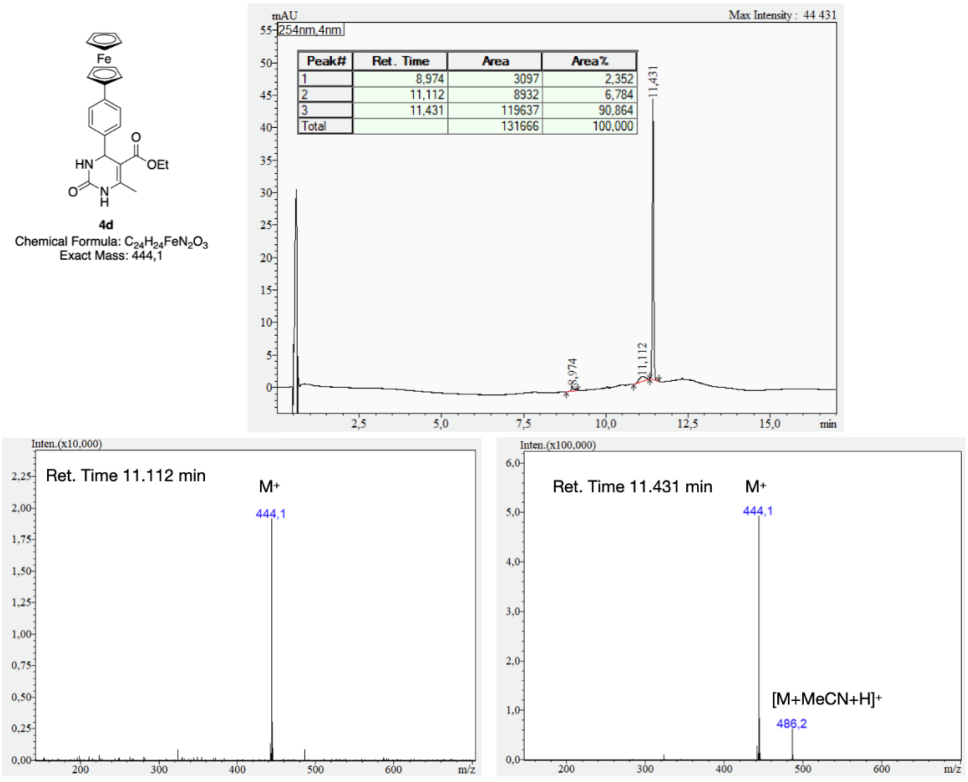

Supporting Figure S46. LC-MS analysis of 4d.

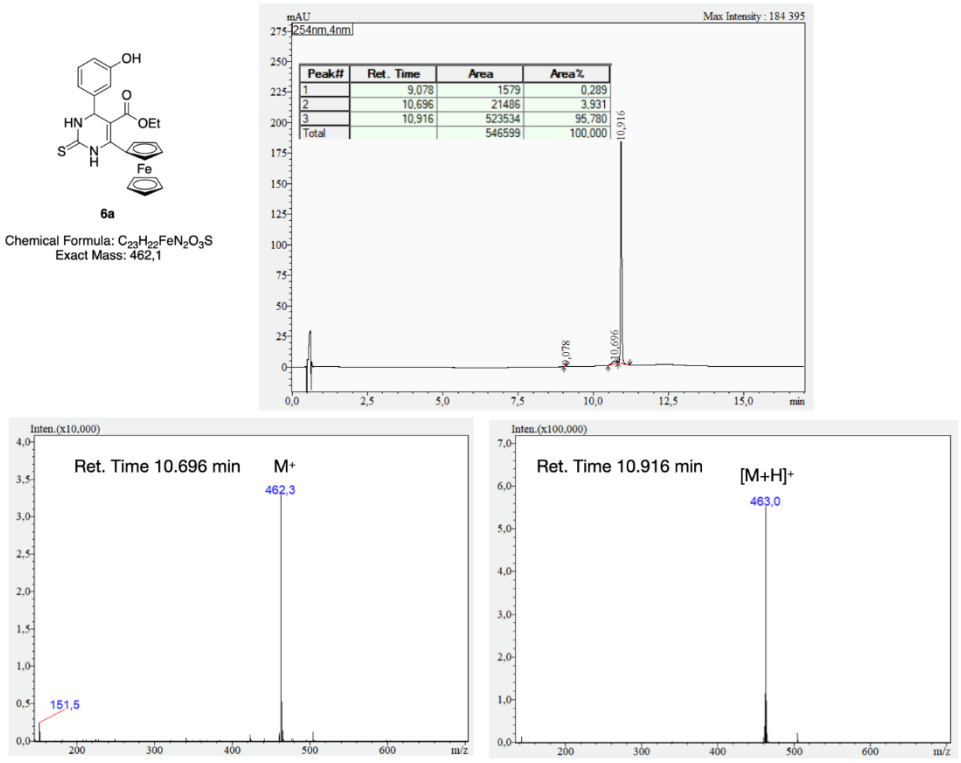

Supporting Figure S47. LC-MS analysis of 6a.

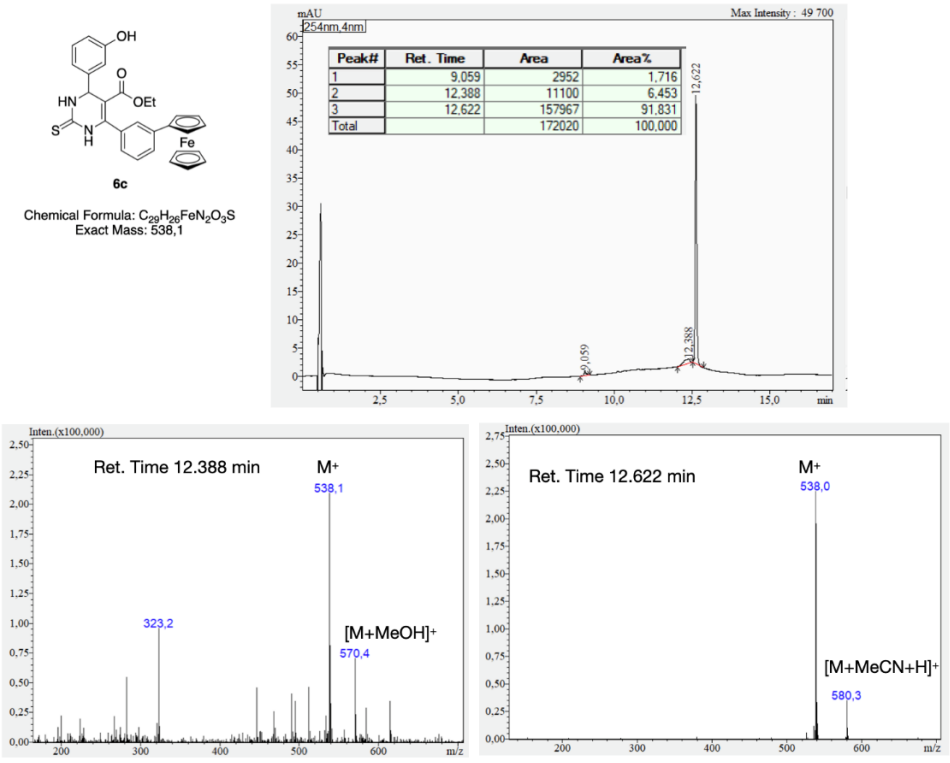

Supporting Figure S48. LC-MS analysis of 6c.

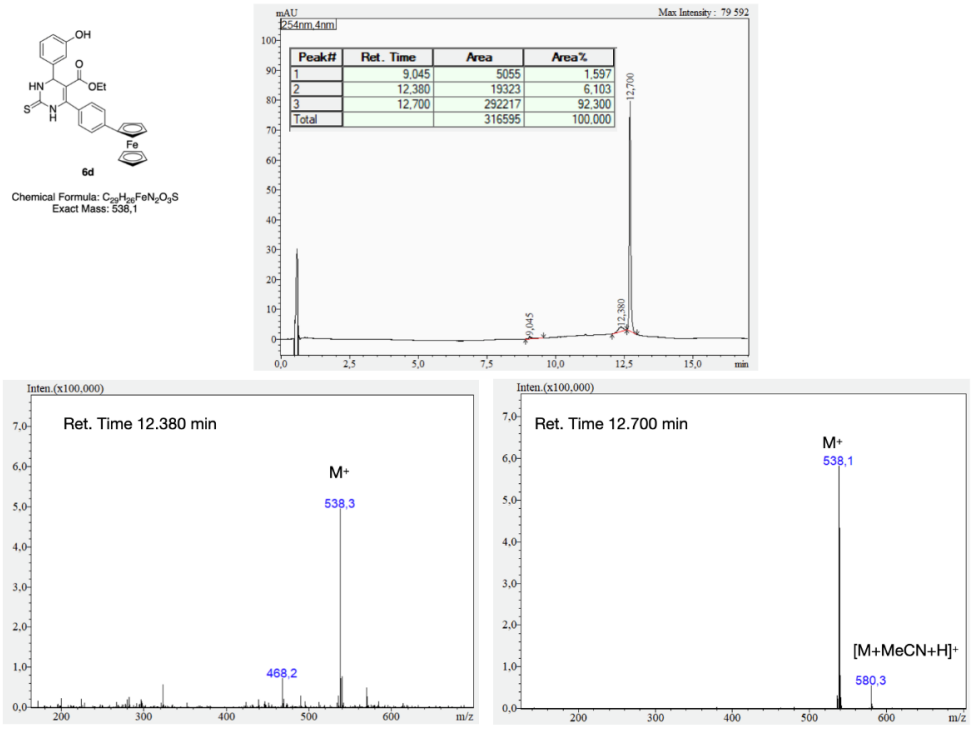

Supporting Figure S49. LC-MS analysis of 6d.

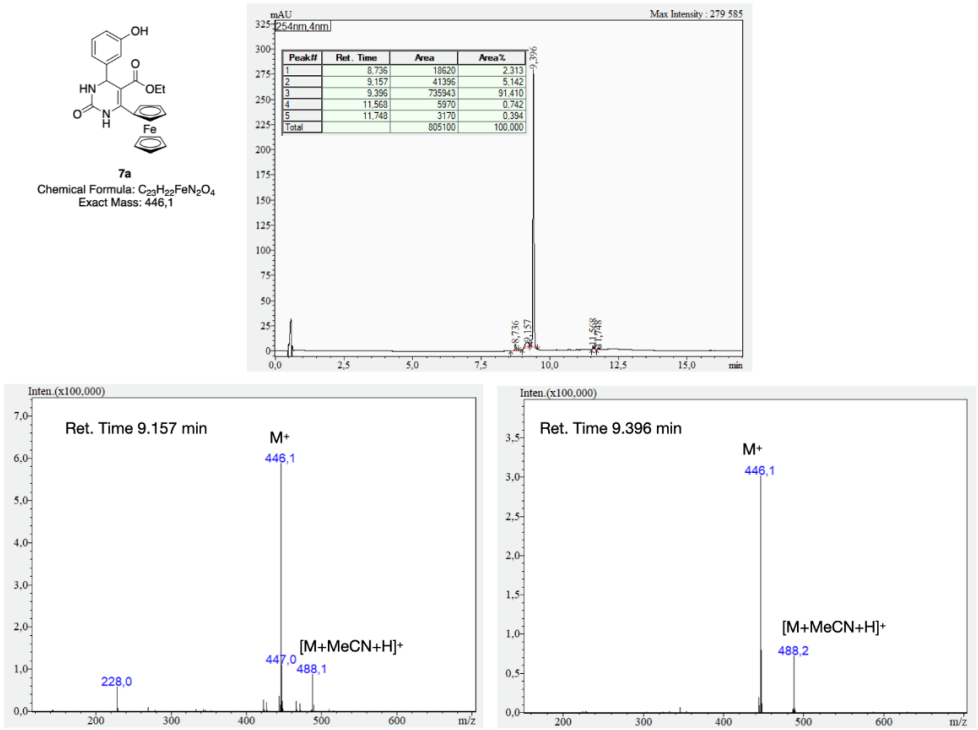

Supporting Figure S50. LC-MS analysis of 7a.

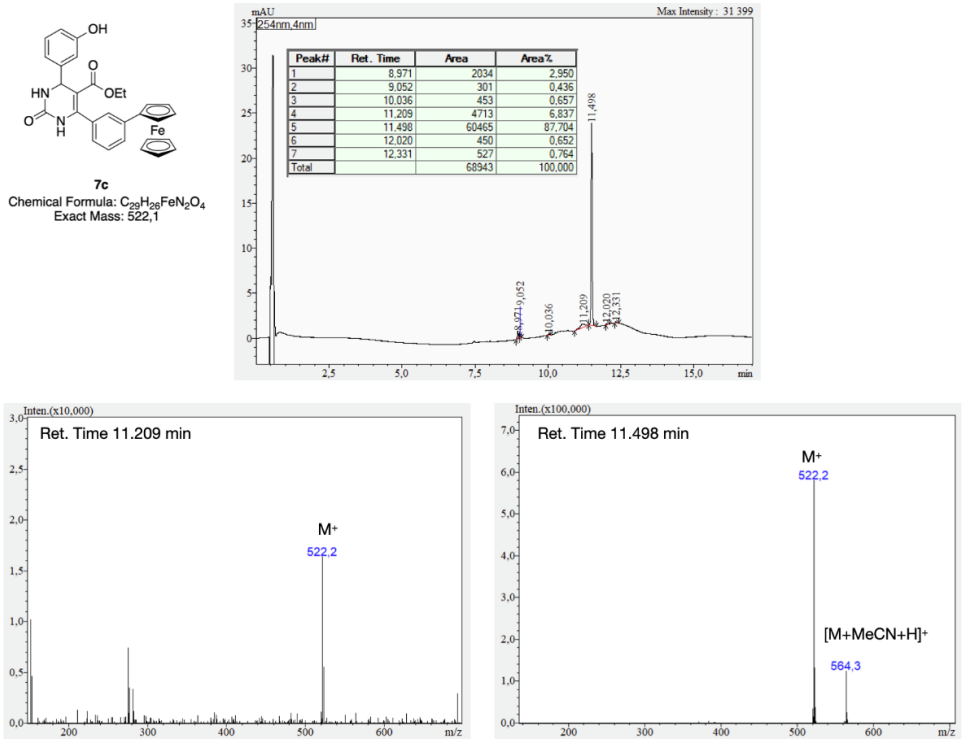

Supporting Figure S51. LC-MS analysis of 7c.

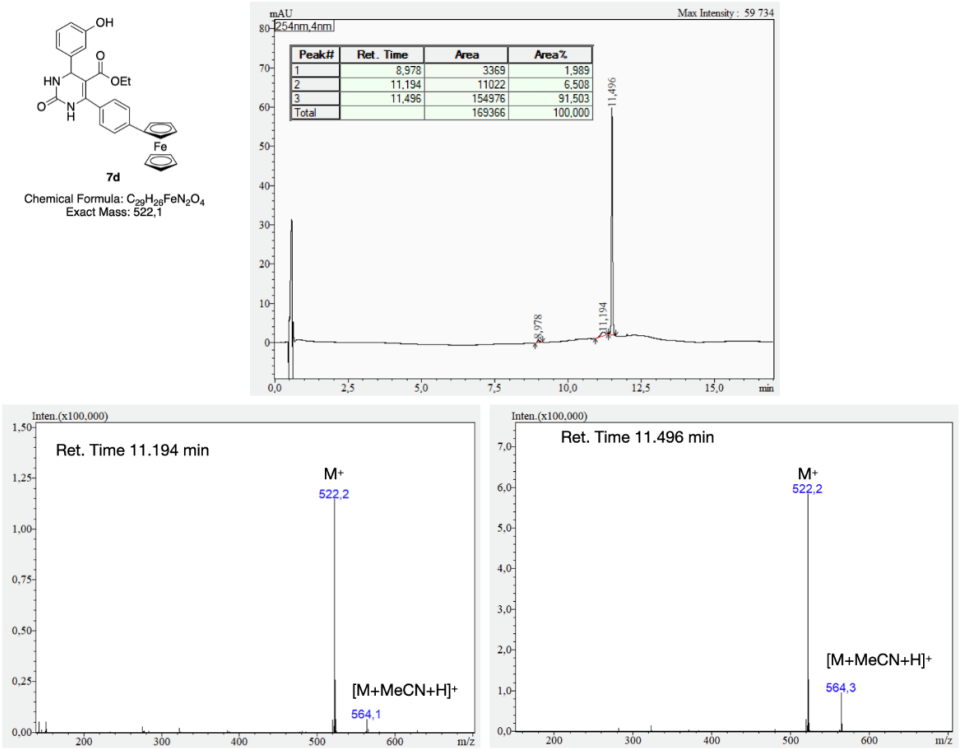

Supporting Figure S52. LC-MS analysis of 7d.

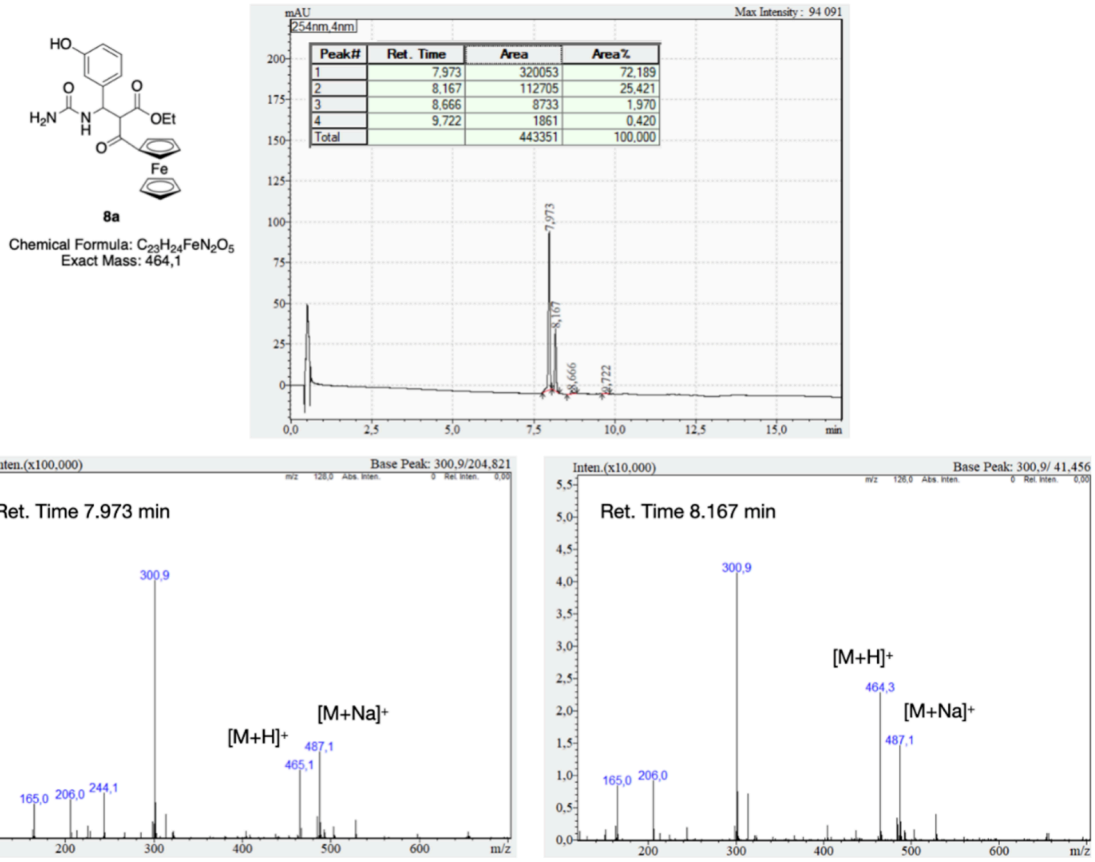

Supporting Figure S53. LC-MS analysis of 8a.

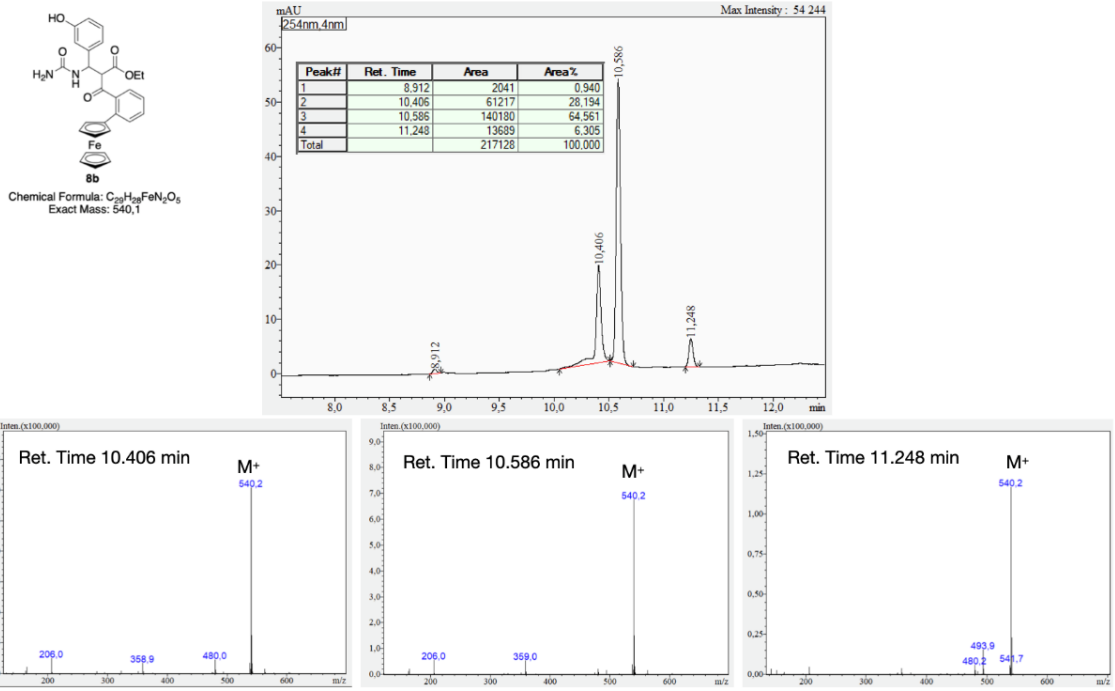

Supporting Figure S54. LC-MS analysis of 8b.

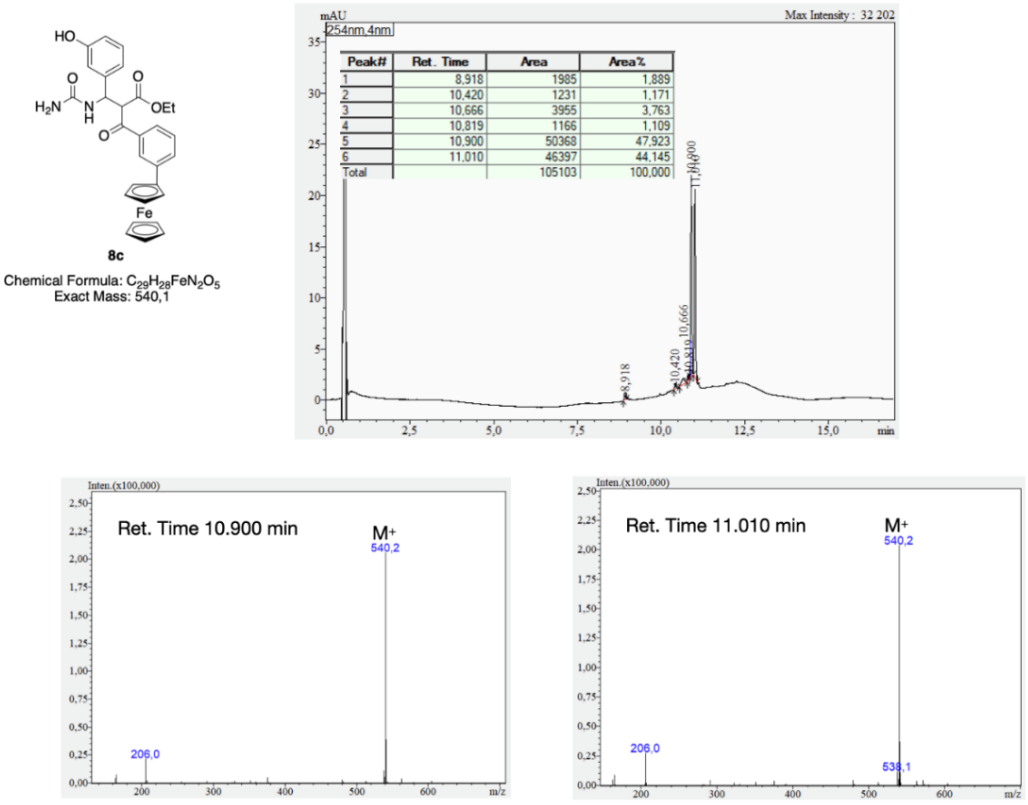

Supporting Figure S55. LC-MS analysis of 8c.

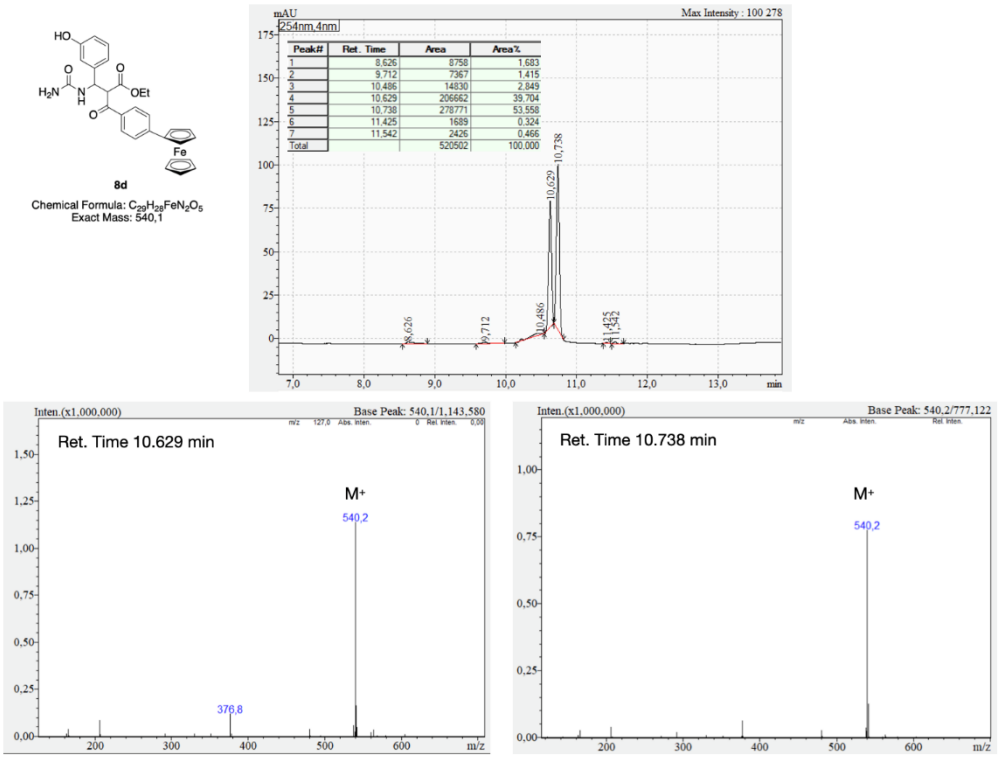

Supporting Figure S56. LC-MS analysis of 8d.

References

1. Yan, Y.; Sardana, V.; Xu, B.; Homnick, C.; Halczenko, W.; Buser, C. A.; Schaber, M.; Hartman, G. D.; Huber, H. E.; Kuo, L. C., Inhibition of a mitotic motor protein: where, how, and conformational consequences. *J. Mol. Biol.* **2004,** *335* (2), 547-54.
2. Garcia-Saez, I.; DeBonis, S.; Lopez, R.; Trucco, F.; Rousseau, B.; Thuéry, P.; Kozielski, F., Structure of human Eg5 in complex with a new monastrol-based inhibitor bound in the R configuration. *J. Biol. Chem.* **2007,** *282* (13), 9740-9747.
3. Soumyanarayanan, U.; Bhat, V. G.; Kar, S. S.; Mathew, J. A., Monastrol mimic Biginelli dihydropyrimidinone derivatives: synthesis, cytotoxicity screening against HepG2 and HeLa cell lines and molecular modeling study. *Org. Med. Chem. Lett.* **2012,** *2* (1), 23.